

UNIVERSIDADE FEDERAL DE VIÇOSA

**Desenvolvimento de um coquetel de bacteriófagos para o controle de
Salmonella enterica in vitro e in vivo utilizando *Aquarana catesbeiana***

Isabella Ribeiro Rodrigues
Magister Scientiae

**VIÇOSA - MINAS GERAIS
2026**

ISABELLA RIBEIRO RODRIGUES

Desenvolvimento de um coquetel de bacteriófagos para o controle de *Salmonella enterica in vitro* e *in vivo* utilizando *Aquarana catesbeiana*

Dissertação apresentada à Universidade Federal de Viçosa, como parte das exigências do Programa de Pós-Graduação em Biologia Celular e Estrutural, para obtenção do título de *Magister Scientiae*.

Orientador: Sergio Oliveira de Paula

**VIÇOSA - MINAS GERAIS
2026**

**Ficha catalográfica elaborada pela Biblioteca Central da Universidade
Federal de Viçosa - Campus Viçosa**

T

R696d
2026
Rodrigues, Isabella Ribeiro, 1999-
Desenvolvimento de coquetel de bacteriófagos para
controle de *Salmonella enterica in vitro* e *in vivo* utilizando
Aquarana catesbeiana / Isabella Ribeiro Rodrigues. – Viçosa,
MG, 2026.

1 dissertação eletrônica (82 f.): il. (algumas color.).

Texto em inglês.

Orientador: Sérgio Oliveira de Paula.

Dissertação (mestrado) - Universidade Federal de Viçosa,
Departamento de Biologia Geral, 2026.

Referências bibliográficas: f. 70- 82.

DOI: <https://doi.org/10.47328/ufvbbt.2026.289>

Modo de acesso: World Wide Web.

1. Bacteriófagos. 2. *Salmonella enterica*. 3. Controle
biológico. 4. *Aquarana catesbeiana*. I. Paula, Sérgio Oliveira
de, 1976-. II. Universidade Federal de Viçosa. Departamento de
Biologia Geral. Programa de Pós-Graduação em Biologia
Celular e Estrutural. III. Título.

CDD 22. ed. 579.26

ISABELLA RIBEIRO RODRIGUES

Desenvolvimento de um coquetel de bacteriófagos para o controle de *Salmonella enterica in vitro* e *in vivo* utilizando *Aquarana catesbeiana*

Dissertação apresentada à Universidade Federal de Viçosa, como parte das exigências do Programa de Pós-Graduação em Biologia Celular e Estrutural, para obtenção do título de *Magister Scientiae*.

APROVADA: 25 de fevereiro de 2026.

Assentimento:

Isabella Ribeiro Rodrigues
Autora

Sergio Oliveira de Paula
Orientador

Essa dissertação foi assinada digitalmente pela autora em 23/06/2026 às 14:40:53 e pelo orientador em 23/06/2026 às 14:47:17. As assinaturas têm validade legal, conforme o disposto na Medida Provisória 2.200-2/2001 e na Resolução nº 37/2012 do CONARQ. Para conferir a autenticidade, acesse <https://siadoc.ufv.br/validar-documento>. No campo 'Código de registro', informe o código **KQ6G.K92A.NZGQ** e clique no botão 'Validar documento'.

AGRADECIMENTOS

Agradeço primeiramente a Deus por me ajudar em todos os obstáculos encontrados ao longo de todos esses anos do mestrado.

Agradeço especialmente minha mãe Keila e minha avó Graça e toda a minha família, por sempre me apoiarem e acreditarem em mim.

Agradeço também a todos os meus amigos que me acompanharam nesta jornada, estejam eles próximos ou à distância. Agradeço também ao meu namorado João, que me apoiou em todos os momentos.

Agradeço ao laboratório de Imunovirologia Molecular da UFV por todo aprendizado durante esses anos de estágio e mestrado pelo auxílio para o meu desenvolvimento como pesquisadora, especialmente a Paloma, não apenas pela orientação, ensinamentos e puxões de orelha, mas também pela amizade.

Agradeço ao Roberto pelo apoio, pelas valiosas orientações e pela constante disponibilidade em me auxiliar ao longo desta jornada.

Agradeço ao professor Oswaldo pela disponibilidade em ceder o espaço da ranicultura para a realização deste trabalho, bem como pelos ensinamentos sobre o manejo das rãs e pela atenção e disponibilidade em auxiliar sempre que necessário.

Agradeço ao professor Sérgio por me receber no laboratório todos esses anos e me dar todo apoio estrutural e orientações necessárias para o desenvolvimento deste trabalho.

Este trabalho foi realizado com o apoio das seguintes agências de pesquisa brasileiras: Coordenação de Aperfeiçoamento de Pessoal de Nível Superior – Brasil (CAPES) – Código de Financiamento 001, Fundação de Amparo à Pesquisa do Estado de Minas Gerais (FAPEMIG) e Conselho Nacional de Desenvolvimento Científico e Tecnológico (CNPq).

RESUMO

RODRIGUES, Isabella Ribeiro, M.Sc., Universidade Federal de Viçosa, fevereiro de 2026. **Desenvolvimento de um coquetel de bacteriófagos para o controle de *Salmonella enterica in vitro* e *in vivo* utilizando *Aquarana catesbeiana*.** Orientador: Sergio Oliveira de Paula.

A ranicultura brasileira destaca-se como uma atividade aquícola de relevância econômica, contudo, a presença de *Salmonella enterica* representa um desafio crítico à saúde pública e à biossegurança do sistema produtivo. Devido ao caráter assintomático da infecção em anfíbios e ao crescimento da resistência antimicrobiana, estratégias de biocontrole, como a terapia fágica, tornam-se alternativas promissoras. Este estudo teve como objetivo desenvolver e avaliar a eficácia de um coquetel de bacteriófagos no controle de *Salmonella Enteritidis in vitro* e *in vivo* utilizando a rã-touro (*Aquarana catesbeiana*). Foram isolados e caracterizados dois bacteriófagos (UFVSen15 e UFVSmin65), sendo o coquetel formulado por esses isolados e pelo bacteriófago UFVCit2, um fago de *Citrobacter* com atividade lítica contra *Salmonella Enteritidis*. Os fagos se mantiveram estáveis ao longo de uma ampla gama de valores de pH e temperaturas. Os ensaios *in vivo* foram realizados em rãs com três faixas de peso corporal: 10–20 g, 80–100 g e 300–350 g. Os resultados demonstraram que o coquetel fágico reduziu significativamente a carga bacteriana na água em todas as fases, com reduções atingindo até 2,53 logs. Nos animais jovens (10–20 g), observou-se uma diminuição de 1,2 log na colonização cloacal. Nas fases de maior peso, a bactéria não foi detectada na cloaca, embora persistisse na água dos grupos controle, reforçando o papel das rãs como portadoras assintomáticas. O coquetel manteve elevada estabilidade na água das caixas das rãs ao longo de todo o período experimental. Conclui-se que o uso de bacteriófagos é uma ferramenta eficaz e sustentável para o biocontrole de *Salmonella* na ranicultura, contribuindo para a redução da contaminação cruzada e o fortalecimento da segurança alimentar sob a perspectiva de Saúde Única.

Palavras-chave: *Salmonella* Enteritidis; bacteriófagos; biocontrole; coquetel; ranicultura

ABSTRACT

RODRIGUES, Isabella Ribeiro, M.Sc., Universidade Federal de Viçosa, February, 2026. **Development of a bacteriophage cocktail for the control of *Salmonella enterica in vitro* and *in vivo* using *Aquarana catesbeiana*.** Adviser: Sergio Oliveira de Paula.

The Brazilian frog farming industry stands out as an aquaculture activity of economic relevance; however, the presence of *Salmonella enterica* represents a critical challenge to public health and production system biosecurity. Due to the asymptomatic nature of infection in amphibians and the increasing antimicrobial resistance, biocontrol strategies such as phage therapy have emerged as promising alternatives. This study aimed to develop and evaluate the efficacy of a bacteriophage cocktail for the control of *Salmonella* Enteritidis *in vitro* and *in vivo* using the bullfrog (*Aquarana catesbeiana*).

Two bacteriophages (UFVSen15 and UFVSmin65) were isolated and characterized, and the cocktail was formulated using these isolates together with bacteriophage UFVCit2, a *Citrobacter* phage with lytic activity against *Salmonella* Enteritidis. The phages remained stable over a wide range of pH values and temperatures.

The *in vivo* assays were conducted using frogs in three body weight ranges: 10–20 g, 80–100 g, and 300–350 g. The results demonstrated that the phage cocktail significantly reduced bacterial loads in the water at all developmental stages, with reductions reaching up to 2.53 log units. In young animals (10–20 g), a 1.2 log reduction in cloacal colonization was observed. In the higher weight groups, the bacterium was not detected in the cloaca, although it persisted in the water of the control groups, reinforcing the role of frogs as asymptomatic carriers. The cocktail maintained high stability in the water of the frog tanks throughout the entire experimental period.

In conclusion, the use of bacteriophages represents an effective and sustainable tool for the biocontrol of *Salmonella* in frog farming, contributing to the reduction of cross-contamination and strengthening food safety from a One Health perspective.

Keywords: *Salmonella* Enteritidis; bacteriophages; biocontrol; cocktail; raniculture

SUMÁRIO

1. INTRODUCTION.....	7
2. OBJECTIVES.....	11
3. MATERIALS AND METHODS.....	12
3.1. Bacterial Strains and Culture Conditions.....	12
3.2. Isolation of Bacteriophages.....	13
3.3. Host Range.....	13
3.4 Efficiency of Plating (EOP).....	14
3.5. Morphology analysis.....	14
3.6. One-step growth curves.....	15
3.7. Thermal and pH stability.....	16
3.8. Multiplicity of Infection influence.....	17
3.9. Bacteriophage Cocktail Formulation.....	17
3.10. Evaluation of the Influence of Multiplicity of Infection on Cocktail Efficiency.....	18
3.11. Efficacy of the Bacteriophage Cocktail in an Animal Model.....	18
3.12. Light Microscopy.....	20
3.13 DNA Extraction, Sequencing, and Genome Assembly.....	20
3.13.1 DNA Extraction and Sequencing.....	20
3.13.2 Genome Annotation, Analysis, and Taxonomic Evaluation.....	21
3.14. Statistical analysis.....	22
4. RESULTS.....	23
4.1. Isolation of Bacteriophages.....	23
4.2 Host Range.....	24
4.3 Efficiency of Plating (EOP).....	26
4.4 Transmission Electron Microscopy (TEM).....	28
4.5. One-Step Growth Curve.....	29
4.6. Thermal and pH stability.....	29
4.7 Influence of Multiplicity of Infection (MOI).....	31
4.8.1. Evaluation of Multiplicity of Infection on Phage Cocktail Efficiency.....	35
4.8.2. Effect of the Phage Cocktail on Bacterial Growth on Agar Plates.....	36
4.9. Efficacy of the Phage Cocktail in an Animal Model.....	37
4.10. Light Microscopy.....	44
4.12. Genome analysis.....	56
4.13. Taxonomic assessment and phylogenetics.....	57
5. DISCUSSION.....	60
6. CONCLUSIONS.....	69
REFERENCES.....	70

1. INTRODUCTION

Salmonella spp. is a genus of gram-negative, rod-shaped bacteria belonging to the family Enterobacteriaceae, recognized worldwide as important etiological agents of salmonellosis (Akiba et al., 2011). The genus comprises more than 2,500 serotypes, divided into the species *Salmonella bongori* and *Salmonella enterica*, the latter being responsible for the majority of infections in humans and animals (Arrach et al., 2008). *S. enterica* is further subdivided into six subspecies: *S. enterica* subsp. *enterica*, *S. enterica* subsp. *salamae*, *S. enterica* subsp. *arizonae*, *S. enterica* subsp. *diarizonae*, *S. enterica* subsp. *houtenae*, and *S. enterica* subsp. *indica* (Porwollik et al., 2004). Among these, *S. enterica* subsp. *enterica* harbors the majority of pathogenic serovars of clinical and epidemiological relevance (Issenhuth-Jeanjean et al., 2014).

Salmonella infection can range from mild cases of gastroenteritis to severe septicemia, depending on the serotype involved, the infectious dose, and the host's immune status (Keestra et al., 2015). The main symptoms of the disease include abdominal pain, fever, and inflammation of the digestive tract (Abd El-Ghany, 2020). Transmission in humans occurs primarily through the consumption of food contaminated with feces, particularly animal-derived products such as meat, eggs, milk, and dairy products, as well as through the ingestion of contaminated water (WHO, 2023; Huang et al., 2022). This scenario results in a high number of foodborne disease outbreaks worldwide, generating significant impacts on public health and the productive sector (Herikstad et al., 2002; Havelaar et al., 2015).

The widespread distribution of this bacterium across different animal groups, including birds, swine, cattle, reptiles, amphibians, and even domestic animals, underscores its zoonotic nature and epidemiological significance (Bruce et al., 2011). Salmonellosis is, therefore, a globally relevant zoonosis, with significant health and economic impacts, particularly in agricultural and aquaculture systems, due to the bacterium's ability to colonize and persist in the gastrointestinal tract of a wide range of hosts (Jajere, 2019; Galán-Relaño et al., 2023).

Although *Salmonella* is more frequently associated with birds and swine, its recurrent presence in amphibians and reptiles highlights these groups as important reservoirs and potential sources of zoonotic transmission (Chen et al., 2010; Guerra et al., 2010; Gorski et al., 2013). Chambers & Hulse (2006) reported that the serovars *Salmonella Typhimurium* and *Salmonella Enteritidis* account for more than 36% of isolates from these animals.

Among amphibians, the bullfrog (*Aquarana catesbeiana*) plays a prominent role, as it often serves as an asymptomatic carrier of *Salmonella* (Silva et al., 2025). In aquaculture environments, this characteristic facilitates the silent dissemination of the bacterium in water, substrate, and among animals, increasing the risk of environmental contamination and transmission to other organisms, including humans (Costa et al., 2021; Ribas & Poonlaphdecha, 2017). Thus, the presence of *Salmonella* in frog farming systems represents not only an animal health issue but also a public health concern, situating raniculture within the epidemiological context of this zoonosis (Cantlay et al., 2017; Hoelzer et al., 2011).

In parallel with this health issue associated with the widespread persistence of *Salmonella* in diverse hosts and environments, there is an alarming increase in bacterial resistance to antimicrobials, a phenomenon primarily linked to the indiscriminate use of antibiotics in human and veterinary medicine, as well as their use as growth promoters in animal production (Bumstead & Barrow, 1993; Odey et al., 2024). This scenario has driven the search for alternative and sustainable strategies for controlling bacterial pathogens, particularly in animal and aquaculture production systems, where selective pressure from antibiotic use is high (Sulakvelidze et al., 2001; Abedon et al., 2011).

In this context, phage therapy has reemerged as a promising biotechnological tool for the targeted control of bacterial pathogens such as *Salmonella* spp. (Danis-Wlodarczyk et al., 2021). Bacteriophages, or phages, are viruses that exclusively infect bacteria and are considered the most abundant biological entities on the planet, with estimates ranging from 10^{31} to 10^{32} viral particles distributed across virtually all ecosystems (Srinivasiah et al., 2008;

Lin et al., 2017). These viruses exhibit high specificity for their bacterial hosts, a characteristic that allows for directional control of pathogens without harming the host's beneficial microbiota (Clokier et al., 2011).

Scientific interest in bacteriophages dates back to the late 19th century, when Ernest Hankin observed that waters from the Ganges and Yamuna rivers displayed bactericidal activity against *Vibrio cholerae* (Hankin, 1896). Later, in 1915, Frederick Twort described a filtrable agent capable of destroying bacterial cultures, a finding that was further consolidated in 1917 by Félix d'Herelle, who coined the term "bacteriophage" when describing the formation of lysis plaques in bacterial cultures (Ackermann, 1987). In the following decades, phages were extensively studied as therapeutic agents; however, the discovery of penicillin in 1928 and the subsequent success of antibiotics led to a decline in interest in phage therapy in Western countries (Kutter, 2004).

Currently, with the rise of antimicrobial resistance, phage therapy has been rediscovered and applied across various fields, including human and veterinary medicine, animal production, aquaculture, and agronomy (Hesse et al., 2019; Svircev et al., 2018). Phages have been experimentally used to control several pathogens, such as *Staphylococcus aureus*, *Escherichia coli*, *Pseudomonas aeruginosa*, and *Salmonella* spp., demonstrating significant efficacy (Singla et al., 2015; Boucher et al., 2022; Zulk et al., 2022).

From a biological perspective, phages are obligate intracellular parasites that utilize the bacterial metabolic machinery for replication (Wittebole et al., 2014). Their typical structure consists of a protein capsid that protects the genetic material, usually double-stranded DNA, a tail responsible for injecting the viral genome into the bacterial cell, and tail fibers that recognize specific receptors on the host surface (Ackermann, 1998). Following adsorption and genome injection, the phage life cycle can proceed along two pathways: the lytic cycle, in which rapid viral replication is followed by bacterial lysis, or the lysogenic cycle, in which the viral genome integrates into the bacterial chromosome as a prophage (Young, 2013; Erez

et al., 2017).

For therapeutic applications, strictly lytic phages are preferred, as they promote the immediate destruction of bacterial cells, exhibiting high replication rates and efficiency in controlling pathogen populations (Weigel & Seitz, 2006). This characteristic makes phages particularly attractive for use in aquaculture and animal production systems, such as raniculture, where targeted pathogen control is desirable without compromising the host's intestinal microbiota (Carvalho et al., 2025; Albarella et al., 2025).

Considering the importance of *Salmonella enterica* as a zoonotic pathogen, the health relevance of the bullfrog as an asymptomatic reservoir, and the growing concern of antimicrobial resistance, the use of bacteriophages emerges as a promising, sustainable, and specific alternative for controlling this bacterium in raniculture systems (Alomari et al., 2021).

Thus, this study proposes the development and application of a bacteriophage cocktail specific for *Salmonella enterica*, evaluating its efficacy in both *in vitro* and *in vivo* assays using *Aquarana catesbeiana*, with the aim of contributing to health management in aquaculture systems and reducing the zoonotic risk associated with salmonellosis.

2. OBJECTIVES

General objective

- To isolate, characterize, and develop a bacteriophage cocktail for the control of *Salmonella enterica in vitro* and *in vivo* using *Aquarana catesbeiana*.

Specific Objectives

- Isolation of bacteriophages for *S. enterica*;
- Biological characterization of the phages: host range, electron microscopy, influence of multiplicity, one-step growth curve, and stability assays.
- Formulation of a bacteriophage cocktail for *in vitro* and *in vivo* application using *Aquarana catesbeiana*.

3. MATERIALS AND METHODS

3.1. Bacterial Strains and Culture Conditions

For this study, bacterial strains were used for the isolation and characterization of phages, as described in Table 1. The bacteria were obtained from the microorganism collection of the Molecular Immunovirology Laboratory at the Federal University of Viçosa (LIVM-UFV), and kindly donated by Professor Ricardo Yamatogi and a partner company, and were cultured in Luria-Bertani (LB) medium (10 g/L NaCl, 10 g/L peptone, and 5 g/L yeast extract) at 37°C under agitation at 180 rpm.

Table 1. Bacterial strains used in this study.

Strain	Identification	Source	Gram Stain
<i>Salmonella</i> Typhimurium	ATCC 14028	-	-
<i>Salmonella</i> Enteritidis	ATCC 13076	-	-
<i>Salmonella</i> 1,4,[5],1:-:1,2	-	Swine	-
<i>Salmonella</i> Cerro	-	Swine	-
<i>Salmonella</i> Panama	-	Swine	-
<i>Salmonella</i> Infantis	-	Swine	-
<i>Salmonella</i> Derby	-	Swine	-
<i>Salmonella</i> Heidelberg	63623	Poultry	-
<i>Salmonella</i> Heidelberg	65499	Poultry	-

<i>Salmonella</i> Mbandaka	64166	Poultry	-
<i>Salmonella</i> Mbandaka	64188	Poultry	-
<i>Salmonella</i> Minnesota	64303	Poultry	-
<i>Salmonella</i> Minnesota	65374	Poultry	-
<i>Citrobacter freundii</i>	ATCC 8090	-	-
<i>Escherichia coli</i>	30	Bovine mastitis	-
<i>Staphylococcus aureus</i>	046	Bovine mastitis	+
<i>Shigella flexneri</i>	ATCC 12022	-	-

3.2. Isolation of Bacteriophages

The phages UFVSen15 and UFVSmin65 were isolated from domestic sewage and chicken litter, respectively, in the municipality of Viçosa (Minas Gerais, Brazil), following the protocol of Van Twest and Kropinski (2009). Briefly, the samples were centrifuged for 10 minutes at $10,000 \times g$ at 4°C to remove solid particles. The resulting supernatant was then filtered through sterile $0.22 \mu\text{m}$ filters. For enrichment, 0.1 mL of the previously cultured host bacterium was added to 5 mL of 2X LB medium (20 g/L NaCl, 20 g/L peptone, and 10 g/L yeast extract) supplemented with 2 mM CaCl_2 (0.22 g/L), and inoculated with 5 mL of the filtered sample. The tubes were subsequently incubated for approximately 24 hours at 37°C with shaking at 100 rpm. After incubation, the samples were centrifuged and filtered again into a new sterile tube.

3.3. Host Range

To determine the host range, i.e., to verify whether the bacteriophage exhibits lytic activity against bacteria other than the host used for its isolation, a spot test was performed.

For this purpose, 0.9 μL of each target bacterium at a concentration of approximately 10^7 CFU/mL was added to 5 mL of molten semi-solid LB medium (0.7% agar) and overlaid onto Petri dishes containing solid LB agar (1.5% agar). After approximately 10 minutes, once the medium had solidified, 10 μL of the phage lysate was pipetted onto the medium containing the bacteria, and the plates were incubated overnight at 37°C . The plates were then examined, and those showing a positive result (presence of lysis zones at the site of spotting) were subjected to the double agar layer plaque assay (Adams, 1959) and incubated overnight again. To ensure viral isolation, this process was repeated until only a single plaque morphology was observed on the same plate. The isolated phages were stored at 4°C for future assays.

3.4 Efficiency of Plating (EOP)

The efficiency of plating (EOP) was used to determine the viral host range and to more comprehensively assess productive infection in *S. enterica* strains, in addition to the original host bacterium. For this purpose, phage lysates were serially diluted and plated onto the susceptible bacteria using the double agar layer plaque assay. To determine the EOP, the average PFU/mL on the test bacterium was divided by the average PFU/mL on the original host bacterium. The EOP evaluation for a specific phage–bacterium combination was defined as follows: “high production” when the ratio was 0.5 or greater (≥ 0.5), indicating that productive infection in the target bacterium yielded at least 50% of the PFU observed for the original host; “medium production” when the EOP ranged from 0.2 to 0.49; “low production” when the EOP ranged from 0.001 to 0.199; and “inefficient” when the EOP was equal to or less than 0.001, according to Khan Mirzai et al. (2015).

3.5. Morphology analysis

The isolated phages were previously concentrated using 10% (w/v) PEG 8000, according to the protocol described by Sambrook et al. (1989) with modifications. Briefly, 30 μL of DNase (10 mg/mL) and RNase (10 mg/mL) were added to every 300 mL of the isolated

phage suspension, followed by incubation at room temperature for 30 minutes. Subsequently, 17.52 g of NaCl was added to the solution, which was kept on ice for 1 hour. The mixture was then centrifuged at $9,000 \times g$ at 4°C for 10 minutes to remove cellular debris. The supernatant was transferred to a sterile tube, and 10% (w/v) PEG 8000 was added; the solution was slowly dissolved and left to stand for 48 hours. After this period, the precipitated phage particles were recovered by centrifugation at $9,000 \times g$ at 4°C for approximately 30 minutes, and the supernatant was discarded. The pellet was resuspended in 7 mL of SM buffer (5.8 g/L NaCl, 2.8 g/L MgSO_4 , 6.057 g/L Tris-HCl, and 0.1 g/L gelatin) using Pasteur pipettes. An equal volume of chloroform was then added to the suspension, which was centrifuged at $9,000 \times g$ at 4°C for 15 minutes; the aqueous fraction containing the phages was subsequently recovered.

For visualization of the isolated phage particles, transmission electron microscopy (TEM) was employed. For this purpose, 10 μL of phage UFVSen15 was applied to Formvar-coated grids. After five minutes, excess liquid was removed with absorbent paper, and the sample was contrasted with 2% uranyl acetate solution for 15 seconds. The samples were kept in a desiccator until analysis using a Zeiss EM 109 transmission electron microscope at the Microscopy and Microanalysis Center of the Federal University of Viçosa (NMM). The obtained images were analyzed for capsid and tail dimensions using ImageJ software.

3.6. One-step growth curves

A one-step growth curve was performed to determine the infection dynamics, including the latent period and burst size of the phages. For this assay, 10 mL of the previously cultured host bacterium, adjusted to an approximate concentration of 10^7 CFU/mL, was infected with a phage suspension to achieve a multiplicity of infection (MOI) of 0.0001. The mixture was incubated at 37°C for 10 minutes to allow viral adsorption and then centrifuged at $9,000 \times g$ for 15 minutes to remove unadsorbed phages. The pellet containing

the infected cells was resuspended in 10 mL of LB medium, from which a 100 μ L aliquot was immediately collected to determine the initial phage titer (T_0).

The suspension was incubated at 37°C with constant shaking at 100 rpm for a total of 100 minutes, with 100 μ L aliquots collected every 10 minutes. Samples were immediately plated using the double agar layer method to quantify phage titers. The latent period was defined as the time interval between viral adsorption and the onset of the first burst. Burst size was calculated as the ratio between the maximum phage yield observed at the end of the lytic cycle and the initial phage yield (T_0).

3.7. Thermal and pH stability

The phages used for the development of the cocktail were evaluated for their stability at different pH values and temperatures. In all assays, the final phage concentration was standardized to 1×10^7 PFU/mL, and immediately after treatment, the phage suspensions were diluted in SM buffer, plated, and titrated using the double agar layer method, as described by Adams (1959). All experiments were conducted in triplicate, and the data were analyzed using GraphPad Prism software, version 8.3.

For thermal stability assessment, 100 μ L aliquots of the phage suspension were added to 900 μ L of SM buffer and incubated for 1 hour at 25, 40, 50, 60, and 70°C, and for 5 minutes at 80 and 90°C. An aliquot of the suspension kept at 4°C, without thermal treatment, was used as a control. After the incubation periods, phages were titrated using the double agar layer method.

Stability at different pH values was evaluated by adding 100 μ L of the phage suspension to 900 μ L of SM buffer previously adjusted to pH values ranging from 2 to 12, followed by incubation at 25°C for 1 hour. The suspension maintained at pH 7 was used as a control. After incubation, phages were titrated as described above.

3.8. Multiplicity of Infection influence

To assess the influence of the multiplicity of infection (MOI) of phages UFVSen15 and UFVSmin65 on the growth of susceptible bacteria, bacterial growth curves were evaluated using 96-well polystyrene microplates. The phage was diluted in SM buffer (5.8 g/L NaCl, 2.0 g MgSO₄·7H₂O, 50 mL of 1 M Tris-HCl, 5 mL of 2% gelatin, pH 7.5) and 20 μL was added to 180 μL of bacterial culture (in LB medium) at the beginning of the exponential growth phase (OD₆₀₀ = 0.1) to achieve MOIs of 0.01, 0.1, 1, and 10. Control wells received 20 μL of SM buffer instead of the phage. The microplates were incubated in a Multiskan™ GO spectrophotometer (Thermo Scientific, USA) at 37°C for 24 hours. Bacterial population density (OD₆₀₀) was measured every 15 minutes by reading the absorbance at 600 nm.

3.9. Bacteriophage Cocktail Formulation

The bacteriophage cocktail used in this study was composed of the phages UFVSen15 and UFVSmin65, characterized in the present work, and a third phage previously isolated and characterized by Cunha (2025) in a doctoral thesis. The use of multiple phages in a single preparation aimed to broaden the spectrum of action against *Salmonella* Enteritidis. The phages were combined in equal proportions, with each isolate previously standardized to the same concentration. The final cocktail was prepared to achieve a total concentration of 1×10^9 PFU/mL, as shown in Table 2. The formulation was performed in SM buffer under aseptic conditions with gentle homogenization to preserve the viability and integrity of the viral particles. After formulation, the bacteriophage cocktail was titrated to confirm the final concentration and subsequently used in both *in vitro* and *in vivo* assays.

Table 2. Phage composition of the cocktail.

Cocktail Name	Composition
Cocktail	UFVSen15, UFVSmin65 e Cit2

3.10. Evaluation of the Influence of Multiplicity of Infection on Cocktail Efficiency

To evaluate the effect of the bacteriophage cocktail under different multiplicities of infection (MOI) on bacterial growth, growth curves were analyzed using 96-well polystyrene microplates. The phage was diluted in SM buffer, and 20 μL aliquots of this solution were added to 180 μL of bacterial culture in the early exponential growth phase ($\text{OD}_{600} = 0.1$), cultivated in LB medium, resulting in MOIs of 0.01, 0.1, 1, and 10. Control wells received 20 μL of SM buffer instead of the phage. The microplates were incubated at 37°C for 24 hours in a Multiskan™ GO spectrophotometer (Thermo Scientific, USA), and bacterial density was monitored by measuring absorbance at 600 nm every 15 minutes.

After 24 hours of incubation, a spot test was performed to assess the effect of the bacteriophage cocktail on bacterial growth using Petri dishes containing solid LB medium (1.5% agar). For this assay, 100 μL aliquots from each experimental condition (MOIs) were removed from the microplate, subjected to serial dilutions, and subsequently, 10 μL of each dilution was pipetted onto the Petri dishes, which were incubated for quantification of colony-forming units (CFU/mL).

3.11. Efficacy of the Bacteriophage Cocktail in an Animal Model

To evaluate the efficacy of the bacteriophage cocktail in controlling *Salmonella* Enteritidis under *in vivo* conditions, 108 *Aquarana catesbeiana* individuals were used,

distributed across three body weight ranges (10–20 g, 80–100 g, and 300–350 g). All procedures involving animals were conducted in accordance with the ethical guidelines of the Animal Use Ethics Committee (CEUAP) of Federal University of Viçosa, protocol number 140/2025. Each weight range consisted of three independent replicates, with each replicate formed by four experimental groups of three animals per group, totaling 36 frogs per weight range. Each experimental group was maintained in a polyethylene box containing three animals.

The experimental groups were as follows: Group 1 – Control, maintained with water and feed without the addition of *Salmonella* Enteritidis or bacteriophages; Group 2 – Salmonella, challenged with *Salmonella* Enteritidis added to the feed; Group 3 – Salmonella + Phages, challenged with *Salmonella* Enteritidis added to the feed and treated with the bacteriophage cocktail diluted in water; and Group 4 – Phages, treated only with the bacteriophage cocktail diluted in water, without bacterial exposure.

The *Salmonella* Enteritidis and bacteriophage cocktail suspensions were prepared under sterile conditions, adjusted to the experimental concentrations, and used immediately after preparation. Treatments were administered orally, with the bacterium delivered via feed and the bacteriophages via water, according to the experimental group. After 72 hours of exposure to the treatments, cloacal swabs were collected from each animal under brief manual restraint, and water samples from the housing boxes were also collected. All samples were immediately sent to the laboratory for microbiological analysis. *Salmonella* Enteritidis quantification was performed using the spot test method, while phage concentrations were determined by the double agar layer plaque assay, as described by Adams (1959). Following cloacal sampling, animals were humanely euthanized by deep anesthesia through immersion in an aqueous solution of benzocaine (250 mg/L), followed by anesthetic overdose and confirmation of death. After confirmation of death, three segments of each portion of the small intestine—proximal (duodenum), middle (jejunum), and distal (ileum)—were collected, as well as the entire large intestine, for subsequent histological analysis.

3.12. Light Microscopy

Bullfrogs individuals from experimental groups 1, 2, 3, and 4 ($n = 3$ per group), as previously described, were evaluated after three days of exposure to the respective treatments, in triplicate. Following confirmation of death, the animals were dissected, and segments of the small and large intestines were collected. Intestinal tissues were immediately transferred to Zamboni's fixative solution, where they remained for 48 hours, as described by Stefanini et al. (1967), dehydrated in ascending ethanol solutions (70%, 80%, 90%, and 95%), and embedded in Leica Histo-resin according to the manufacturer's instructions. Sections of 3 μm thickness were obtained using a Leica RM 2245 rotary microtome, stained with hematoxylin (15 min) and eosin (30 s), and subsequently analyzed and photographed using an Olympus BX60 light microscope.

3.13 DNA Extraction, Sequencing, and Genome Assembly

3.13.1 DNA Extraction and Sequencing

Viral DNA was extracted following the PCI/SDS DNA extraction protocol (phagedb.org) with modifications. Briefly, to every 1 mL of lysate, 12.5 μL of 1 M MgCl_2 , 40 μL of 0.5 M EDTA, 5 μL of Proteinase K (10 mg/mL), and 50 μL of 10% SDS were added. The solution was vortexed and incubated at 55°C for 60 minutes. After incubation, an equal volume of PCI solution (phenol, chloroform, and isoamyl alcohol in a 25:24:1 ratio) was added. The mixture was centrifuged at $9,000 \times g$ at 4°C for 10 minutes, and this step was repeated three times to maximize contaminant removal. The aqueous phase was transferred to a new sterile tube, and 1 mL of 95% ethanol and 50 μL of 3 M sodium acetate were added. The tube was then placed on ice for approximately 5 minutes and centrifuged at $9,000 \times g$ at 4°C for 10 minutes. The resulting pellet was washed with 1 mL of 70% ethanol and centrifuged again at $9,000 \times g$ at 4°C for 10 minutes. This washing step was repeated until the pellet became more transparent. Finally, the pellet was air-dried at room temperature for

approximately 20 minutes and resuspended in 50 μ L of autoclaved distilled water. The extracted DNA was stored at -20°C until sequencing.

Viral sequencing was performed by Novogene Corporation Inc. (Sacramento, CA, USA) using the Illumina NovaSeq 6000 platform.

3.13.2 Genome Annotation, Analysis, and Taxonomic Evaluation

The raw sequencing data were submitted to the Bacterial and Viral Bioinformatics Resource Center (PATRIC) (<https://www.bv-brc.org/>) for viral genome assembly using the platform's standard "Assembly Tool" parameters. The resulting contigs were annotated using PATRIC's "Annotation Tool" via the RAST server (<https://rast.nmpdr.org/rast.cgi>). The genomic map of phage UFVSen15 was generated using the Proksee platform (<https://proksee.ca/>).

NCBI Virus BLASTn (<https://www.ncbi.nlm.nih.gov/labs/virus/vssi/#/>) was employed to initiate taxonomic analyses, and related reference sequences (RefSeq) were randomly retrieved corresponding to the contig. The VIRIDIC web server (<https://rhea.icbm.uni-oldenburg.de/viridic/>) and the Viral Proteomic Tree (ViPTree) (<https://www.genome.jp/viptree/>) platforms were used for genomic comparison and phylogenetic relationship assessment of the phages, constructing a proteomic tree among the selected sequences and the contig, respectively. Similarity values obtained from VIRIDIC were interpreted according to ICTV criteria, considering 95% as the species demarcation threshold and 70% for genus-level classification.

VirulenceFinder 2.0 (<https://cge.food.dtu.dk/services/VirulenceFinder/>) was used to screen for potential virulence factors, while ResFinder 4.1 (<https://cge.food.dtu.dk/services/ResFinder/>) was employed to detect antimicrobial resistance genes. The phage genomes were further analyzed for the presence of potential tRNA-encoding genes using the tRNAscan-SE server

(<http://lowelab.ucsc.edu/tRNAscan-SE/>). Finally, the PhageAI server was used to predict the phage life cycle.

3.14. Statistical analysis

All experiments were conducted in triplicate. Data were analyzed using GraphPad Prism version 8.3. In the stability assays, the effect of multiplicity of infection (MOI) was evaluated by one-way analysis of variance (one-way ANOVA), considering a significance level of 95%. For the *in vivo* experiments, differences between groups were further assessed using the unpaired t-test, also performed with the same software.

4. RESULTS

4.1. Isolation of Bacteriophages

After three consecutive propagation cycles using the double agar layer technique, phage isolates with plaques exhibiting uniform morphology were obtained. Phage UFVSen15 was isolated from a wastewater sample using *Salmonella Typhimurium* ATCC 14028 as the host bacterium, whereas phage UFVSmin65 was isolated from a chicken litter sample using *Salmonella Minnesota* 65374 as the host. Plates were incubated at 37°C for 24 hours. The plaques formed by both phages exhibited well-defined edges and no halo; however, UFVSmin65 produced smaller and clearer plaques compared to UFVSen15.

Titration of the isolates, performed after the purification cycles, demonstrated reproducibility of viral titers across successive replicates, with no significant increase in titer observed throughout the propagation cycles. Phage UFVSen15 presented a viral titer of 1.5×10^9 PFU/mL, while UFVSmin65 exhibited a titer of 4.0×10^{10} PFU/mL.

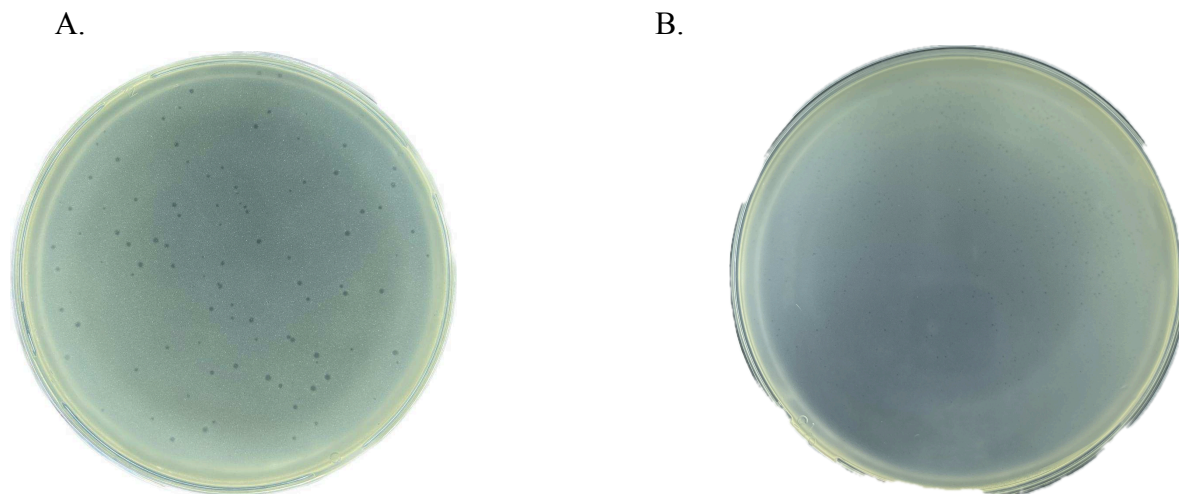


Figure 1. Petri dishes showing bacterial lawns and the formation of lysis plaques by phage UFVSen15 (A) and phage UFVSmin65 (B).

4.2 Host Range

After performing the spot-test to assess host range (Table 3), three types of results were observed: positive (“+”), obtained when the phage disrupts the bacterial lawn and forms clear lysis plaques at the spot; negative (“-”), characterized by normal bacterial growth, i.e., absence of lysis plaques; and partial or inefficient lysis (“+-”), when turbid plaques are formed compared to the positive result.

Phage UFVSen15 exhibited lytic activity against multiple *Salmonella enterica* serovars, including *S. Typhimurium* (the isolation host strain), *S. Enteritidis*, *S. 1,4,[5],12:i:-*, *S. Cerro*, *S. Panama*, *S. Infantis*, *S. Derby*, and *S. Heidelberg* 63623. No lytic activity was observed against *Citrobacter freundii* ATCC 8090, *Shigella flexneri* 12022, *Staphylococcus aureus*, or some other *Salmonella* strains tested.

Phage UFVSmIn65 showed a distinct host range, with lytic activity against its isolation host strain (*Salmonella* Minnesota 65374), *S. Enteritidis*, *S. 1,4,[5],12:i:-*, *S. Cerro*, *S. Panama*, *S. Infantis*, and *S. Derby*, as well as positive lysis against *Escherichia coli* 30. However, no lytic activity was detected against *Citrobacter freundii*, *Shigella flexneri*, or *Staphylococcus aureus*.

Table 3. Host range of the isolated phages.

Strain	Phage UFVSen15	Phage UFVSmIn65
<i>Salmonella</i> Typhimurium	Isolation host	+
<i>Salmonella</i> Enteritidis	+	+

<i>Salmonella</i> 1,4,[5],1:-:1,2	+	+
<i>Salmonella</i> Cerro	+	+
<i>Salmonella</i> Panama	+	+
<i>Salmonella</i> Infantis	+	+
<i>Salmonella</i> Derby 1	+	+
<i>Salmonella</i> Derby 2	+	+
<i>Citrobacter freundii</i> ATCC 8090	-	-
<i>Escherichia coli</i> 30	-	+
<i>Shigella flexneri</i> 12022	-	-
<i>Staphylococcus aureus</i> 046	-	-
<i>Salmonella</i> Heidelberg 63623	+	-
<i>Salmonella</i> Heidelberg 65499	-	-
<i>Salmonella</i> MBandaka 64166	-	-
<i>Salmonella</i> MBandaka 64188	-	-
<i>Salmonella</i> Minnesota 64303	-	-
<i>Salmonella</i> Minnesota 65374	-	Isolation host

4.3 Efficiency of Plating (EOP)

The efficiency of plating (EOP) assay was performed to quantitatively evaluate the results previously classified as positive in the spot-test, characterized by bacterial growth inhibition (+).

Phage UFVSen15 exhibited an EOP of 2.33 against *S. Enteritidis*, being classified as high production, which indicates greater infection efficiency compared to the original host bacterium. EOP values < 0.001 were observed for *S. 1,4,[5],12:i:-* and *S. Heidelberg 63623*. For *S. Panama*, *S. Derby*, *S. Cerro*, and *S. Infantis*, no lysis plaques were formed, resulting in an EOP of 0.

Table 4. Efficiency of plating of phage UFVSen15. High efficiency: EOP 0.5–1.0; moderate efficiency: EOP 0.2– <0.49 ; low efficiency: 0.001– <0.199 ; and inefficient: ≤ 0.001 .

Strain	EOP
<i>Salmonella</i> Typhimurium	1
<i>Salmonella</i> Enteritidis	2,33
<i>Salmonella</i> 1,4,[5],1:-:1,2	0,000000085
<i>Salmonella</i> Heidelberg 63623	0,0000001
<i>Salmonella</i> Panamá	0
<i>Salmonella</i> Derby 1	0
<i>Salmonella</i> Derby 2	0
<i>Salmonella</i> Cerro	0

Salmonella Infantis

0

Phage UFVSmin65 also exhibited greater infection efficiency against *S. Enteritidis* compared to its original host bacterium, with an EOP of 1.14, being classified as high production. Low production infections (0.001–0.199) were observed for *S. Cerro* and *S. Derby 1*. No lysis plaques were formed for *S. Panama*, *S. Derby 2*, *S. 1,4,[5],12:i:-*, *S. Typhimurium*, *S. Infantis*, and *Escherichia coli* 30, resulting in an EOP of 0.

Table 5. Efficiency of plating of phage UFVSmin65. High efficiency: EOP 0.5–1.0; moderate efficiency: EOP 0.2–<0.49; low efficiency: 0.001–<0.199; and inefficient: ≤0.001.

Strain	EOP
<i>Salmonella</i> Minnesota 65374	1
<i>Salmonella</i> Typhimurium	0
<i>Salmonella</i> Enteritidis	1,14
<i>Salmonella</i> 1,4,[5],1:-:1,2	0
<i>Salmonella</i> Cerro	0,00223
<i>Salmonella</i> Panamá	0
<i>Salmonella</i> Infantis	0
<i>Salmonella</i> Derby 1	0,006

<i>Salmonella</i> Derby 2	0
<i>Escherichia coli</i> 30	0

4.4 Transmission Electron Microscopy (TEM)

Transmission electron microscopy revealed that phage UFVSen15 exhibits a myovirus morphology, with an icosahedral capsid approximately 65 nm in diameter, a long tail of approximately 210 nm, and a contractile sheath of about 62 nm. In turn, phage UFVSmin65 also displays a myovirus morphology, presenting an elongated isometric capsid with an approximate diameter of 96.7 nm and a tail of about 88 nm.

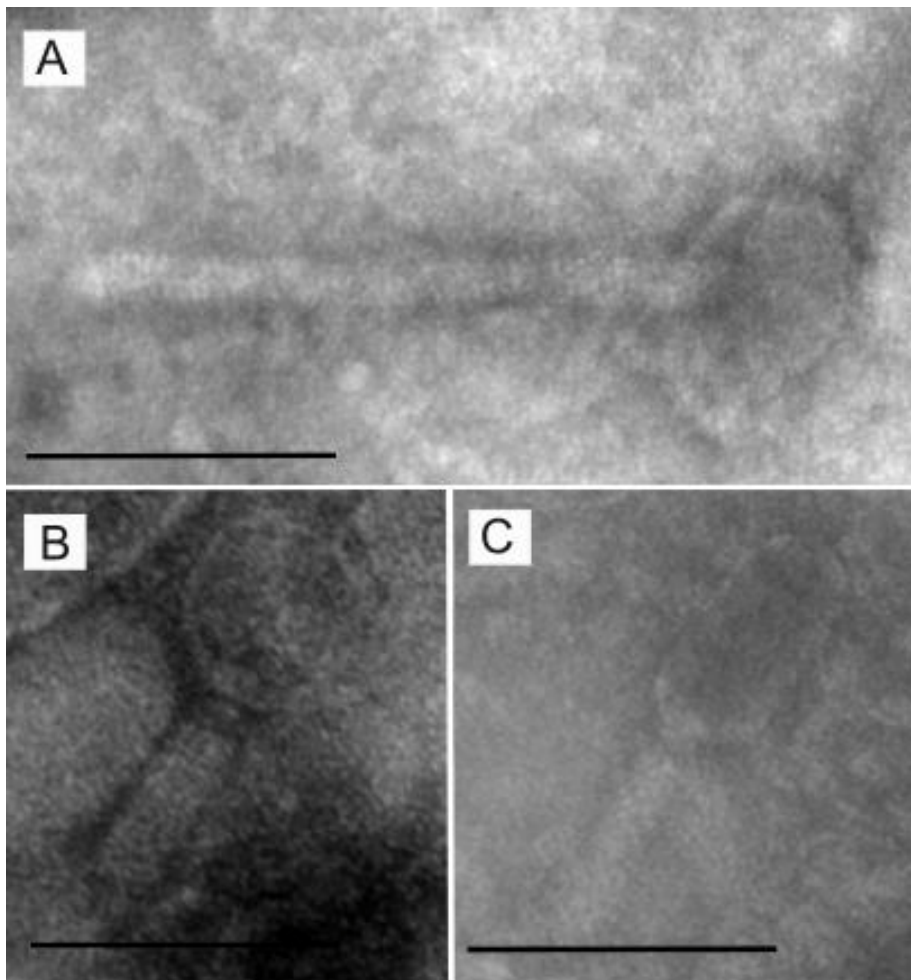


Figure 4. Transmission electron micrographs (TEM) of bacteriophages UFVSen15 and UFVSmin65. (A) UFVSen15 particle with the tail in a relaxed state. (B) UFVSen15 particle

with the contracted tail, highlighting the contractile sheath. (C) UFVSmin65 particle. Scale bars represent 100 nm.

4.5. One-Step Growth Curve

The one-step growth curve revealed that phage UFVSen15 (Figure 5-A) exhibited a latent period of approximately 30 minutes and an average burst size of 254 PFU per cell. In contrast, phage UFVSmin65 (Figure 5-B) displayed a longer latent period (40 minutes) and a lower burst size (19.8 PFU per cell).

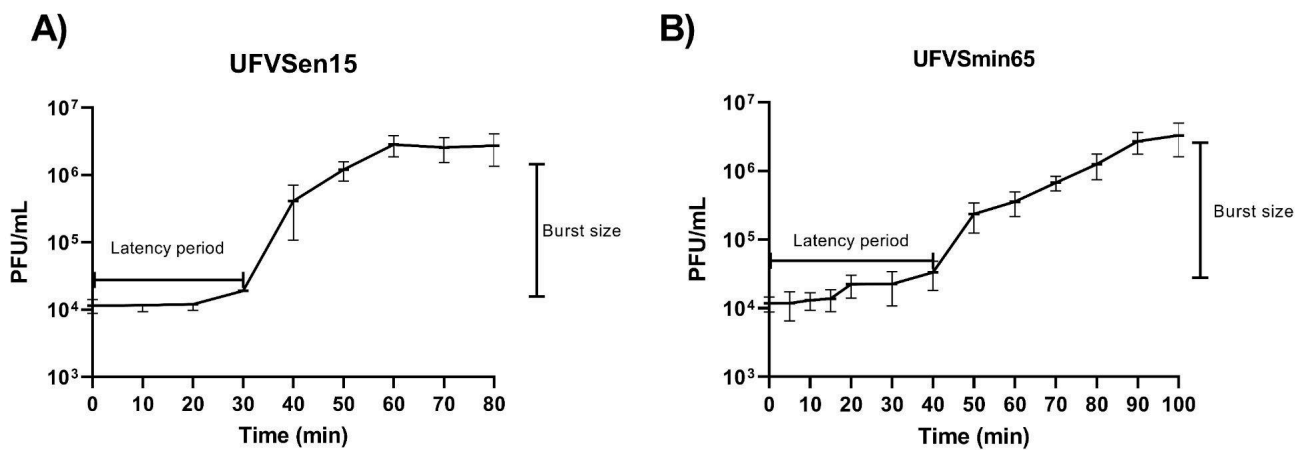


Figure 5. One-step growth curve of phage UFVSen15 (A) and UFVSmin65 (B).

4.6. Thermal and pH stability

An important characteristic of biocontrol agents is their ability to withstand adverse conditions. Accordingly, stability tests were performed with the isolated phages. Phage stability at different pH values was assessed after 24 hours of incubation (Figure 6). UFVSen15 remained stable at pH values ranging from 3 to 12, while complete inactivation was observed at pH 2. For phage UFVSmin65, a similar behavior was observed under acidic and neutral conditions, with complete inactivation at pH 2 and stability maintained between pH 3 and pH 11, showing titers close to 10⁷ PFU/mL. However, at pH 12, a significant

reduction in viability was observed, indicating lower tolerance of this phage to highly alkaline conditions compared to UFVSen15.

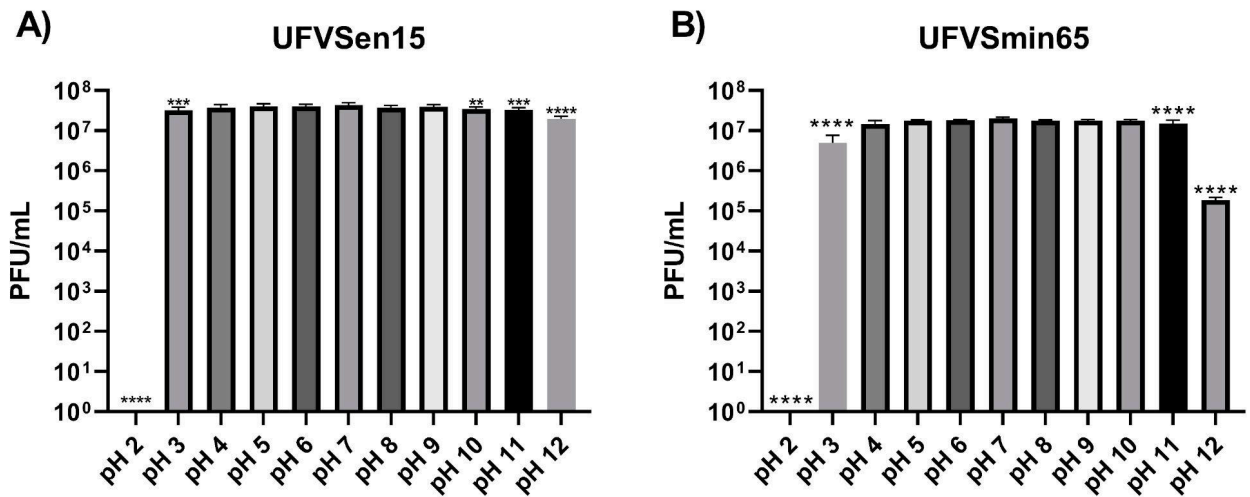


Figure 6. Stability at different pH values for phage UFVSen15 (A) and UFVSmIn65 (B). Statistically significant treatments ($P \leq 0.05$) compared to the control are indicated by * (* $P < 0.05$; ** $P < 0.01$; *** $P < 0.001$; **** $P < 0.0001$).

Thermal stability of the phages was evaluated after 24 hours of incubation at different temperatures (Figure 7). Phage UFVSen15 maintained titers similar to the control between 25 °C and 70 °C. At 80 °C, a significant reduction in viability was observed, while complete inactivation occurred at 90 °C. In contrast, phage UFVSmIn65 showed lower thermal tolerance, remaining stable only between 25 °C and 50 °C. At 60 °C, titers decreased significantly, with a sharp decline at 70 °C and complete inactivation at 80 °C and 90 °C.

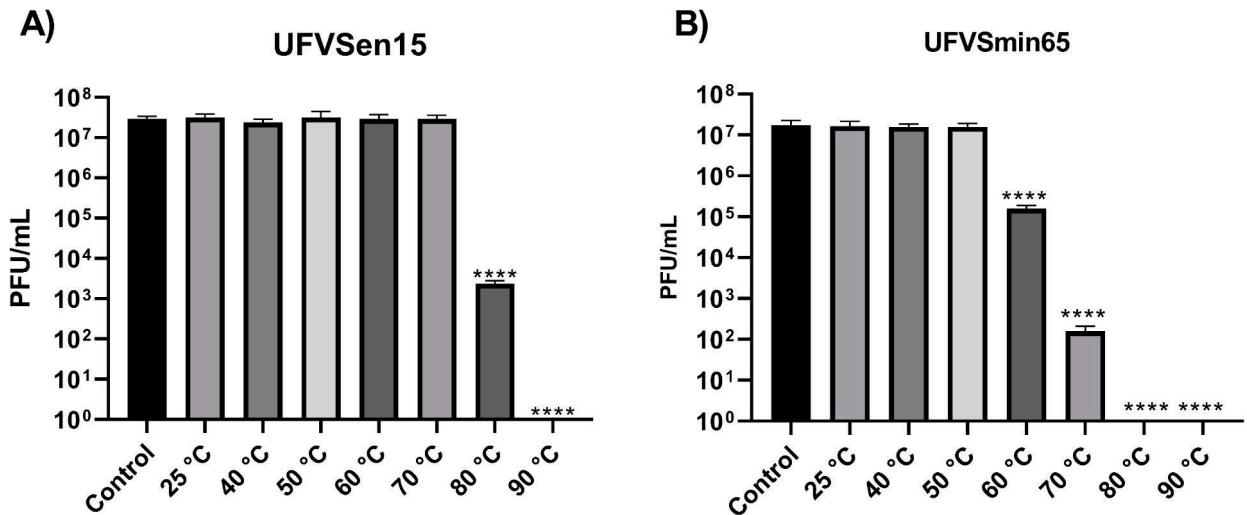


Figure 7. Stability at different temperatures for phage UFVSen15 (A) and UFVSmin65 (B). Statistically significant treatments ($P \leq 0.05$) compared to the control are indicated by * (* $P < 0.05$; ** $P < 0.01$; *** $P < 0.001$; **** $P < 0.0001$).

4.7 Influence of Multiplicity of Infection (MOI)

Bacterial growth curves at different MOIs in the presence of phage UFVSen15 are shown in Figure 2. The phage was able to reduce the growth of its host bacterium, *Salmonella Typhimurium*, as well as the serovars *S. Enteritidis*, *S. Heidelberg 63623*, *S. Infantis*, and *S. 1,4,[5],12:i:-*, with the most pronounced effect observed at MOI 0.01. Growth inhibition did not show a linear relationship with increasing MOI, as higher phage concentrations (MOI 1 and 10) resulted in a lower inhibitory effect, suggesting more efficient infection at lower phage-to-bacterium ratios. The main differences between treated and control curves were observed in the initial growth phases, indicating a delay in the onset of bacterial exponential growth. For some serovars, such as Heidelberg, Infantis, and 1,4,[5],12:i:-, this reduction persisted throughout the experimental period, demonstrating a sustained effect of the phage. In contrast, the serovars Panama, Derby 1, Derby 2, and Cerro exhibited growth curves similar to the control at all MOIs tested, indicating low susceptibility to UFVSen15.

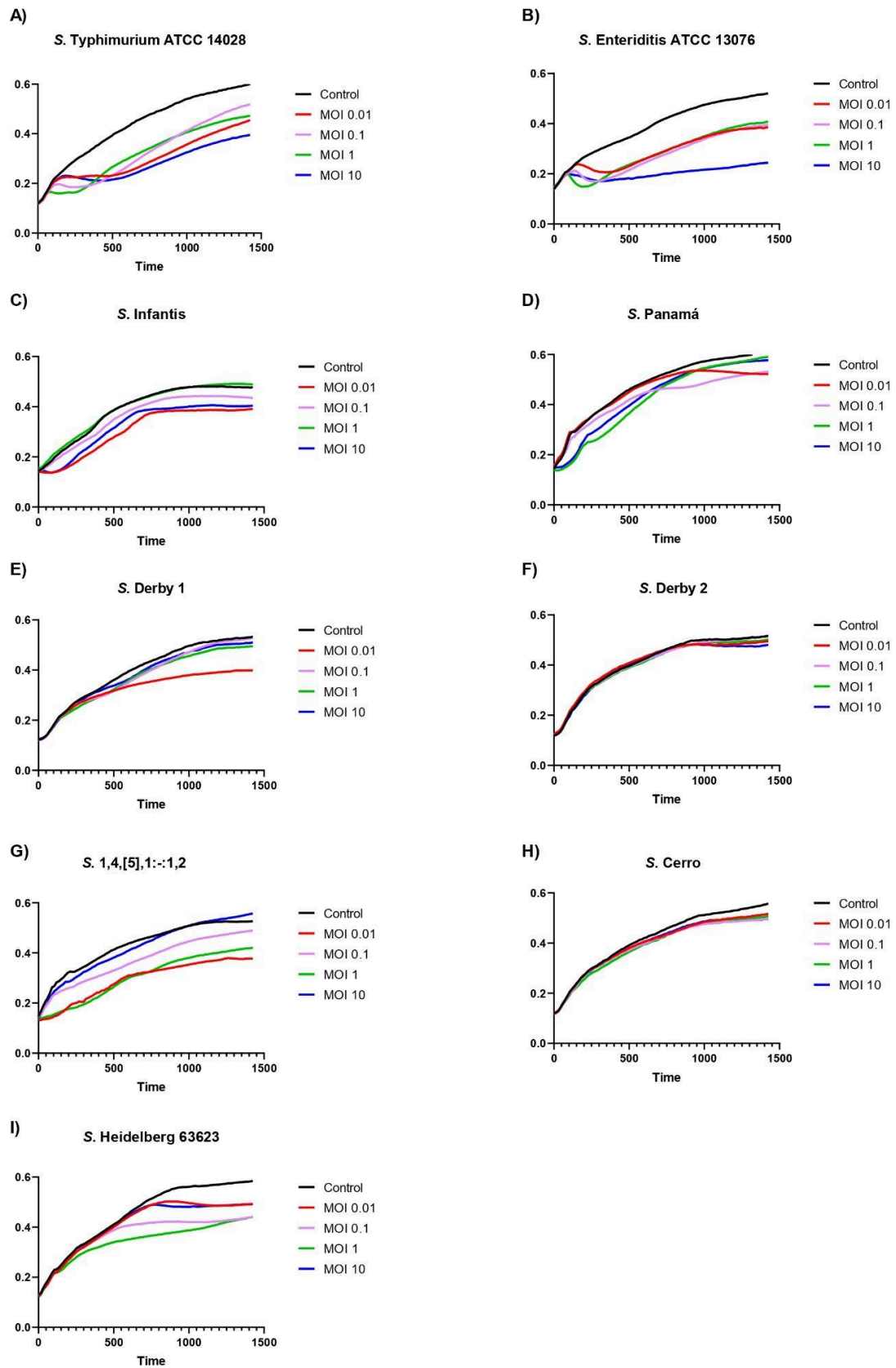


Figure 2. Growth curves of phage UFVSen15 at different MOIs: 0.01, 0.1, 1, and 10 for the bacteria: A) *Salmonella* Typhimurium, B) *Salmonella* Enteritidis, C) *Salmonella* Infantis, D) *Salmonella* Panama, E) *Salmonella* Derby 1, F) *Salmonella* Derby 2, G) *Salmonella*

1,4,[5],12:i:-, H) *Salmonella* Cerro, and I) *Salmonella* Heidelberg 63623. Assays were conducted in 96-well polystyrene plates in triplicate and incubated at 37°C for 24 h.

Bacterial growth curves in the presence of phage UFVSmin65 are shown in Figure 3. Unlike UFVSen15, growth inhibition by UFVSmin65 was clearly MOI-dependent, with MOI 10 producing the greatest reduction in growth for most serovars tested. At lower MOIs (0.01 and 0.1), the curves frequently resembled the control, indicating that a higher phage-to-bacterium ratio was necessary to achieve an inhibitory effect. For several serovars, including Minnesota, Enteritidis, Infantis, 1,4,[5],12:i:-, Cerro, Derby 1, and Derby 2, growth reduction persisted throughout the experimental period, indicating a more sustained bacteriolytic effect compared to UFVSen15. Notably, some serovars with low susceptibility to UFVSen15, such as Derby 1, Derby 2, and Cerro, were sensitive to UFVSmin65, highlighting differences in host range between the phages. Conversely, *S. Typhimurium* showed little variation between treatments and control, indicating lower susceptibility to this phage. Additionally, *E. coli* 30 showed no significant growth reduction at any MOI, confirming the specificity of UFVSmin65 for *Salmonella*.

Given that both phages exhibited inhibitory activity against *S. Enteritidis*, albeit with distinct kinetic behaviors, this serovar was selected for subsequent assays using the phage cocktail.

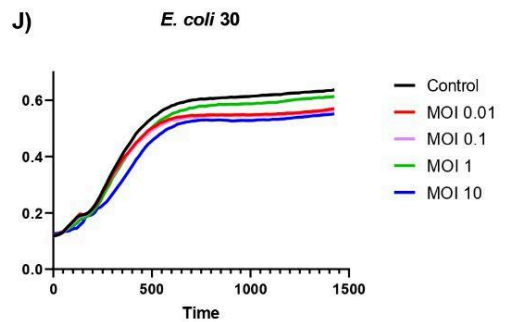
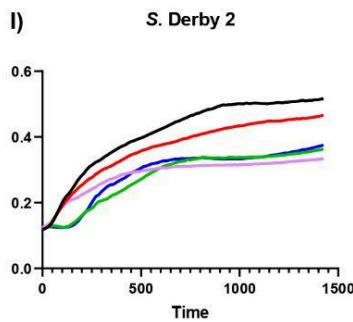
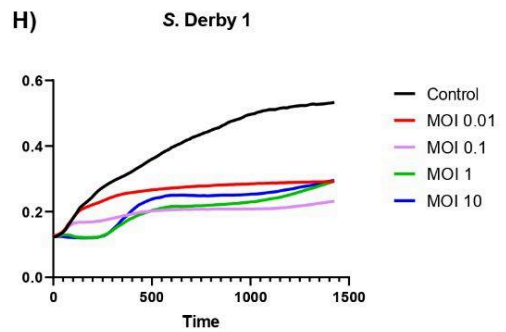
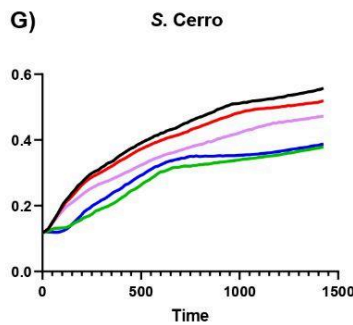
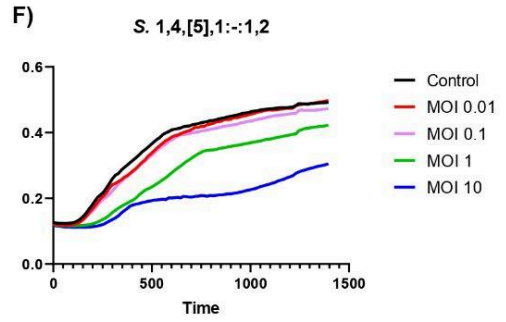
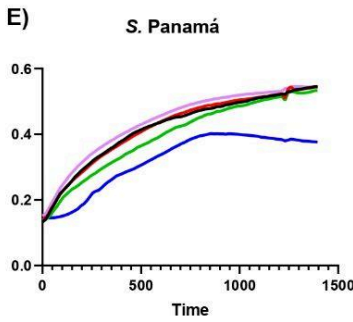
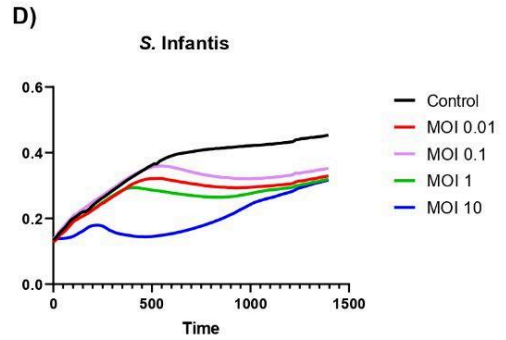
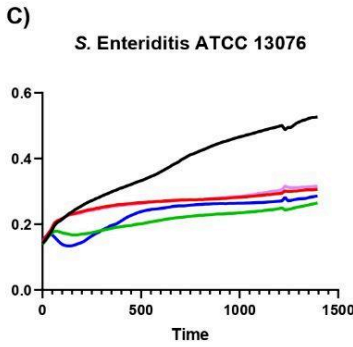
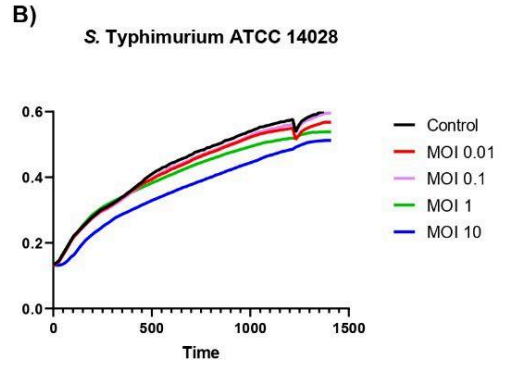
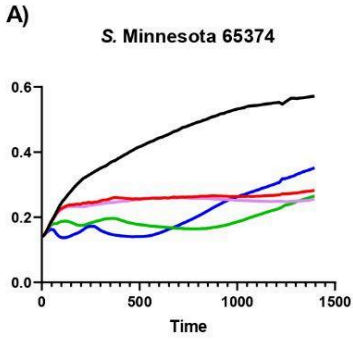


Figure 3. Growth curves of UFVSmin65 at different MOIs: 0.01, 0.1, 1, and 10 for the bacteria: A) *Salmonella* Minnesota 65374 B) *Salmonella* Typhimurium C) *Salmonella* Enteritidis D) *Salmonella* Infantis E) *Salmonella* Panama F) *Salmonella* 1,4,[5],1:-:1,2 G) *Salmonella* Cerro H) *Salmonella* Derby 1 I) *Salmonella* Derby 2 e J) *E.coli* 30. O ensaio foi realizado em placas de 96 poços em triplicata. Assays were conducted in 96-well plates in triplicate and incubated at 37°C for 24 h.

4.8.1. Evaluation of Multiplicity of Infection on Phage Cocktail Efficiency

The phage cocktail evaluated in this study consisted of three phages: two characterized herein (UFVSen15 and UFVSmin65) and a third previously described by Cunha (2025) in a doctoral thesis. The growth curves of *Salmonella* Enteritidis in the presence of the phage cocktail demonstrated a direct influence of multiplicity of infection (MOI) on bacterial growth (Figure 8). All treatments containing phages showed reduced growth compared to the control, confirming the lytic activity of the cocktail throughout the experimental period.

The divergence between treated and control curves was observed from the early stages of the assay, indicating an early inhibition of the bacterial exponential growth phase. Moreover, the effect of the cocktail showed a clear linear relationship with increasing MOI, where higher phage-to-bacterium ratios resulted in more pronounced growth reductions. At lower MOIs (0.01 and 0.1), initial bacterial growth was followed by a slowdown and stabilization at levels below the control. At higher MOIs (1 and 10), growth restriction was more pronounced from the onset of the experiment and remained sustained throughout the 24-hour period.

This kinetic behavior reflects the complementary action of the phages in the cocktail, combining the initial growth delay observed for UFVSen15 with the prolonged inhibitory effect characteristic of UFVSmin65, resulting in higher efficiency in controlling *S. Enteritidis*. The cocktail also contains a third phage previously characterized in another study, which may

further contribute to the observed efficiency.

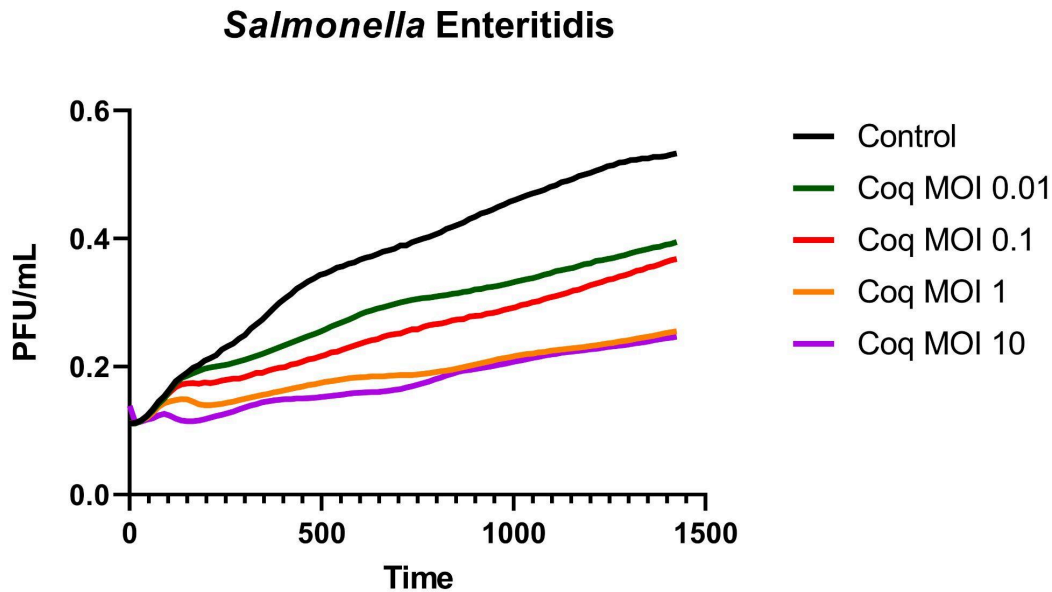


Figure 8. Bacterial growth curves of *S. Enteritidis* over 24 hours in the presence of the phage cocktail at different multiplicities of infection (MOIs): 0.01, 0.1, 1, and 10.

4.8.2. Effect of the Phage Cocktail on Bacterial Growth on Agar Plates

The influence of multiplicity of infection (MOI) on the action of the phage cocktail against *Salmonella* Enteritidis was evaluated through microplate growth curves and confirmed by spot-test after 24 hours (Figure 9). All treatments containing the cocktail significantly reduced bacterial density compared to the control, demonstrating the lytic activity of the phages. Bacterial counts in the control reached approximately 10^9 CFU/mL after 24 hours. For treatments with MOIs of 0.01 and 0.1, a reduction of approximately 1 to 2 logs in CFU/mL was observed. In treatments with MOIs of 1 and 10, the reduction was more pronounced, reaching about 3 logs compared to the control. These results indicate that the inhibitory effect of the phage cocktail is MOI-dependent, with greater bacterial population reductions observed as the phage-to-bacterium ratio increases, confirming the efficiency of the cocktail in controlling *S. Enteritidis* growth in both liquid and solid media.

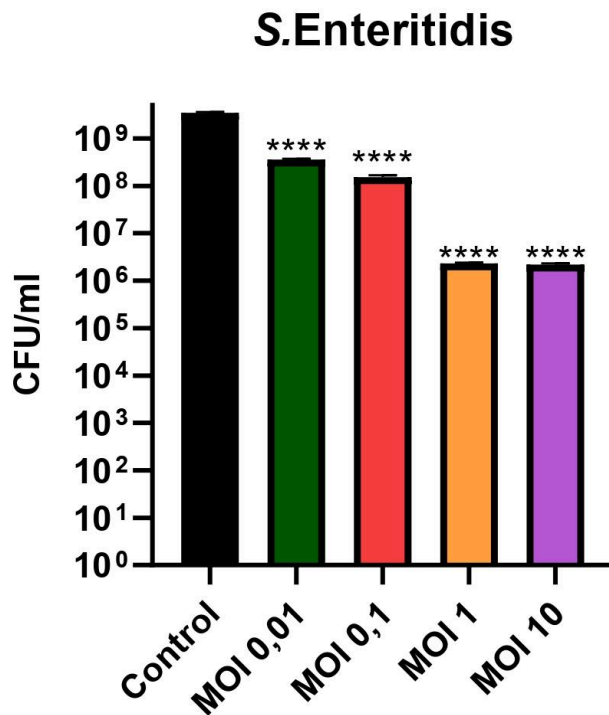


Figure 9. Effect of multiplicity of infection (MOI) of the phage cocktail on *Salmonella* Enteritidis density after 24 hours of incubation, evaluated by spot-test on LB agar. Statistically significant treatments ($P \leq 0.05$) compared to the control are indicated by * (* $P < 0.05$; ** $P < 0.01$; *** $P < 0.001$; **** $P < 0.0001$).

4.9. Efficacy of the Phage Cocktail in an Animal Model

The biocontrol potential of the phage cocktail was evaluated through *in vivo* assays using bullfrogs (*Aquarana catesbeiana*) at three different developmental stages (10–20 g, 80–100 g, and 300–350 g). The objective was to assess the treatment's capacity to reduce *Salmonella* Enteritidis load both within the animals and in the production environment. Intestinal colonization was monitored via cloacal swabs, and bacterial persistence was assessed in the tank water. Additionally, phage particle viability and stability in water were evaluated to ensure that the bioagent remained active under experimental conditions.

In the 10–20 g weight group, the phage cocktail effectively reduced *S. Enteritidis* in

both parameters analyzed (Figure 10). In the intestinal tract (Figure 10A), bacterial counts in the cloaca of the treated group showed a significant reduction of approximately 1.2 logs compared to the control ($P < 0.05$), indicating that the treatment hindered bacterial colonization or persistence in the host. Similarly, bacterial recovery from the tank water (Figure 10B) revealed an even more pronounced reduction, approximately 1.74 logs in the group receiving the cocktail ($P < 0.0001$). These results suggest that the cocktail not only mitigates internal bacterial load in juvenile frogs but also functions as a potent environmental decontaminant, reducing *Salmonella* dissemination in the aquatic ecosystem during early growth stages.

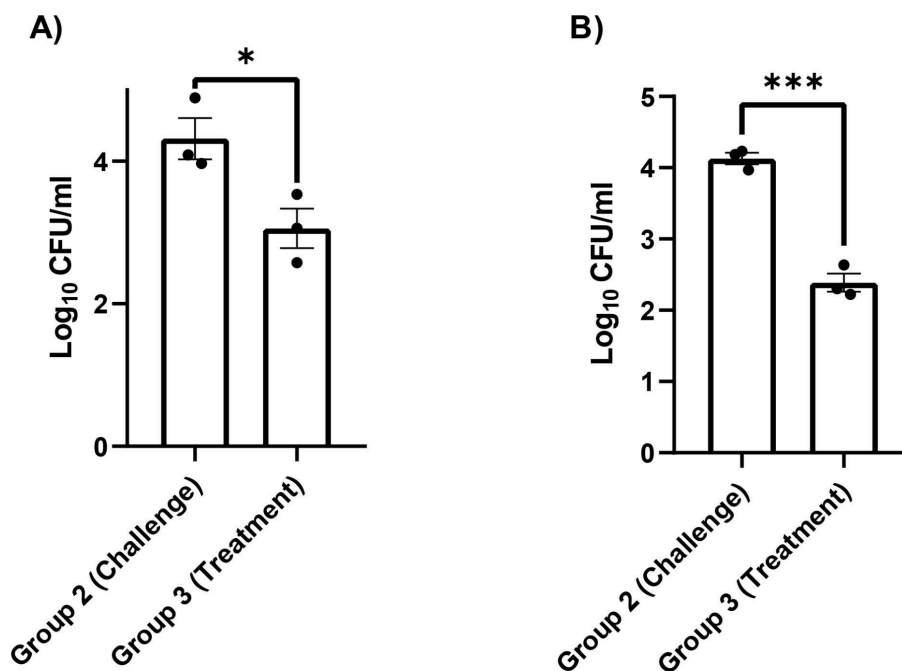


Figure 10. Recovery of *Salmonella* Enteritidis in bullfrogs weighing 10–20 g. (A) Bacterial counts in cloacal swabs; (B) Bacterial recovery from tank water. Bars represent the mean of three independent biological replicates ($n=3$), where in A each tank value corresponds to the mean of three individually sampled animals, and in B to the mean of triplicate technical readings from a single environmental sample. Error bars indicate the standard error of the mean (SEM). Data are expressed as log₁₀ CFU/mL. Groups G1 and G4 had zero counts and were omitted for clarity. Statistically significant differences compared to the control are

indicated by * (* $P < 0.05$; ** $P < 0.01$; *** $P < 0.001$; **** $P < 0.0001$).

Regarding phage cocktail viability in water (Figure 11), no statistically significant difference was observed between groups G3 and G4 ($P = 0.2029$), indicating high phage stability in the aquatic environment, independent of host bacteria presence.

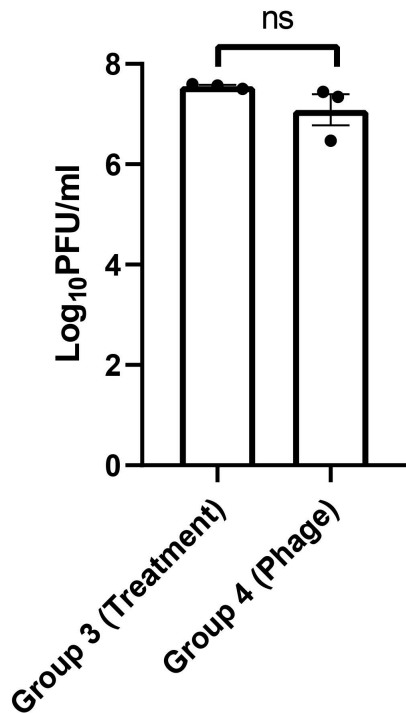


Figure 11. Recovery of the phage cocktail from bullfrog tank water (10–20 g). Bars represent the mean of three independent biological replicates ($n=3$), where each tank value corresponds to the mean of triplicate technical readings from a single environmental sample. Error bars indicate SEM. Data are expressed as \log_{10} CFU/mL. Groups G1 (Negative Control) and G2 (Challenge) were excluded from phage analysis, as they were not inoculated with the cocktail, and prior analyses confirmed the absence of native phages. Statistically significant differences compared to the control are indicated by * (* $P < 0.05$; ** $P < 0.01$; *** $P < 0.001$; **** $P < 0.0001$).

In the 80–100 g weight group, infection dynamics differed from the previous stage. No *S. Enteritidis* was recovered from cloacal swabs in any experimental group, indicating no detectable cloacal colonization under the tested conditions. However, analysis of tank water

(Figure 12) confirmed pathogen persistence in the environment, with the challenge group showing high bacterial counts. Treatment with the phage cocktail resulted in a statistically significant reduction ($P < 0.0001$) of *Salmonella* in water, decreasing environmental contamination levels by approximately 2.2 logs. These results highlight the cocktail's role as a sanitary barrier, demonstrating that even in the absence of animal colonization, the phage cocktail effectively sanitizes the water, reducing the risk of pathogen cross-contamination in the production system.

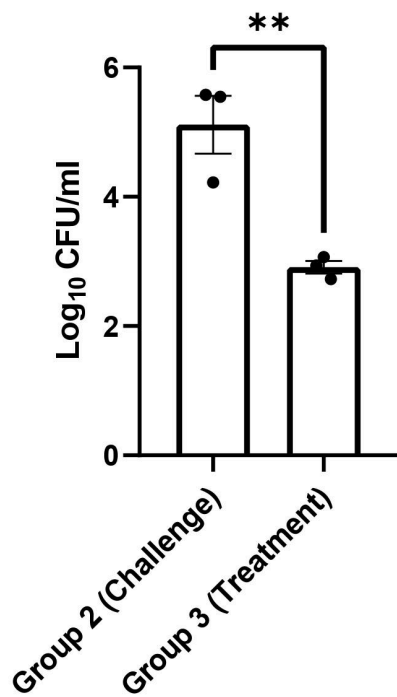


Figure 12. Recovery of *Salmonella* Enteritidis from bullfrog tank water (80–100 g). Bars represent the mean of three independent biological replicates (tanks), with each tank value corresponding to the mean of triplicate technical readings from a single environmental sample ($n=3$). Error bars indicate SEM. Data are expressed as \log_{10} CFU/mL. Groups G1 and G4 had zero counts and were omitted for clarity. Statistically significant differences compared to the control are indicated by * ($*P<0.05$; $**P<0.01$; $***P<0.001$; $****P<0.0001$).

Phage cocktail viability (Figure 13), as observed in the previous weight group, showed no statistically significant difference between groups G3 and G4 ($P = 0.3669$), maintaining viral titers around 10^7 PFU/mL.

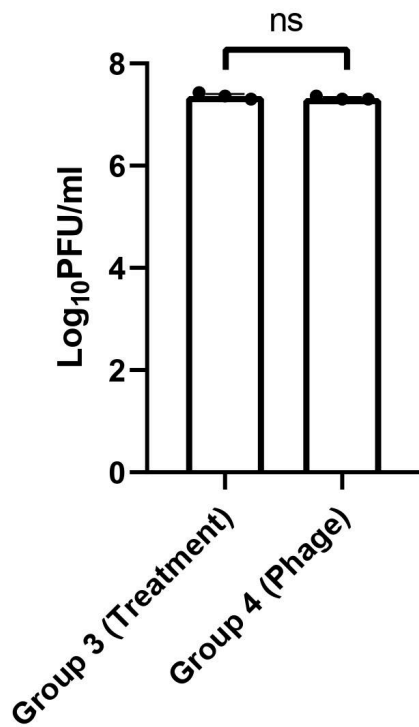


Figure 13. Recovery of the phage cocktail from bullfrog tank water (80–100 g). Bars represent the mean of three independent biological replicates ($n=3$), with each tank value corresponding to the mean of triplicate technical readings from a single environmental sample. Error bars indicate SEM. Data are expressed as \log_{10} CFU/mL. Groups G1 and G2 were excluded from phage analysis. Statistically significant differences compared to the control are indicated by * ($*P<0.05$; $**P<0.01$; $***P<0.001$; $****P<0.0001$).

In the 300–350 g weight group, as in the previous stage, no *S. Enteritidis* was recovered from cloacal swabs in any group, confirming the absence of detectable cloacal colonization in adult animals (Figure 14). Nevertheless, analysis of water contamination revealed a highly significant reduction of approximately 2.53 logs ($P < 0.0001$). These results are consistent with the pattern observed in the previous stage, reinforcing the treatment's efficacy in adult animals.

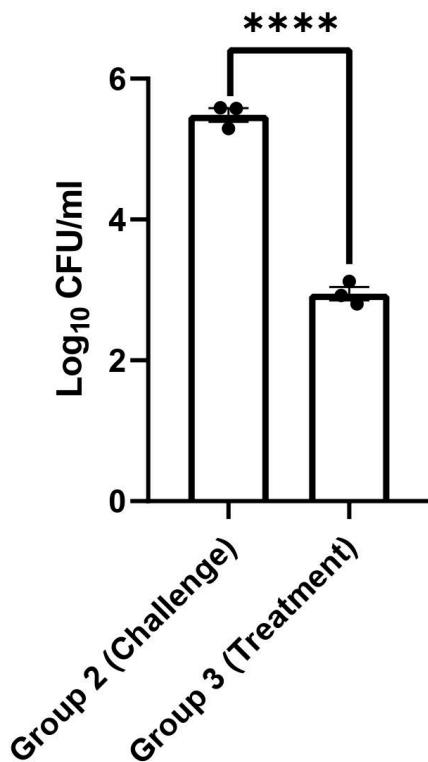


Figure 14. Recovery of *Salmonella* Enteritidis from bullfrog tank water (300–350 g). Bars represent the mean of three independent biological replicates (tanks), with each tank value corresponding to the mean of triplicate technical readings from a single environmental sample ($n=3$). Error bars indicate SEM. Data are expressed as \log_{10} CFU/mL. Groups G1 and G4 had zero counts and were omitted for clarity. Statistically significant differences compared to the control are indicated by * ($*P < 0.05$; $**P < 0.01$; $***P < 0.001$; $****P < 0.0001$).

Phage cocktail viability in water (Figure 15) did not differ significantly between groups G3 and G4 ($P = 0.1985$), with viral titers remaining stable around 10^7 PFU/mL, confirming the persistence and stability of the bioagent in the aquatic environment until the final growth stage.

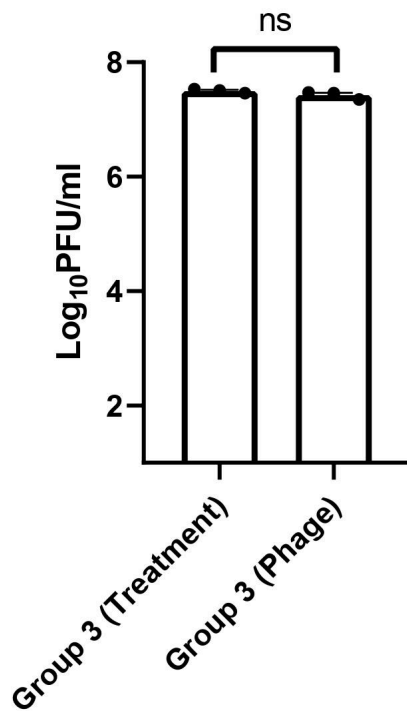


Figure 15. Recovery of the phage cocktail from bullfrog tank water (300–350 g). Bars represent the mean of three independent biological replicates ($n=3$), with each tank value corresponding to the mean of triplicate technical readings from a single environmental sample. Error bars indicate SEM. Data are expressed as \log_{10} CFU/mL. Groups G1 and G2 were excluded from phage analysis. Statistically significant differences compared to the control are indicated by * ($*P<0.05$; $**P<0.01$; $***P<0.001$; $****P<0.0001$).

4.10. Light Microscopy

Histological examination of the evaluated organs, considering all regions analyzed in each, revealed no significant morphological differences among the experimental groups. All regions exhibited a similar structural pattern, with preservation of tissue organization and no evident histopathological alterations. The epithelium displayed a typical morphological pattern, composed of digestive columnar cells, stem cells, goblet cells, and endocrine cells, with intraepithelial lymphocytes present in numbers consistent with normality. Goblet cells showed preserved distribution and morphology, with staining patterns corresponding to the mucus produced in each segment. The striated border was well developed, with appropriate height and length relative to the respective regions, exhibiting a digitiform organization in the small intestine and crypt arrangement in the large intestine. Connective tissue in the lamina propria and submucosa appeared preserved, with fibroblasts and blood vessels clearly visible, along with occasional eosinophils in the large intestine, all within physiological norms. No signs of inflammatory processes were observed, such as a significant increase in leukocytes or diffuse inflammatory infiltrate. The muscular layer exhibited organization and thickness consistent with normality, without discontinuities or structural alterations, maintaining the typical pattern of the analyzed regions.

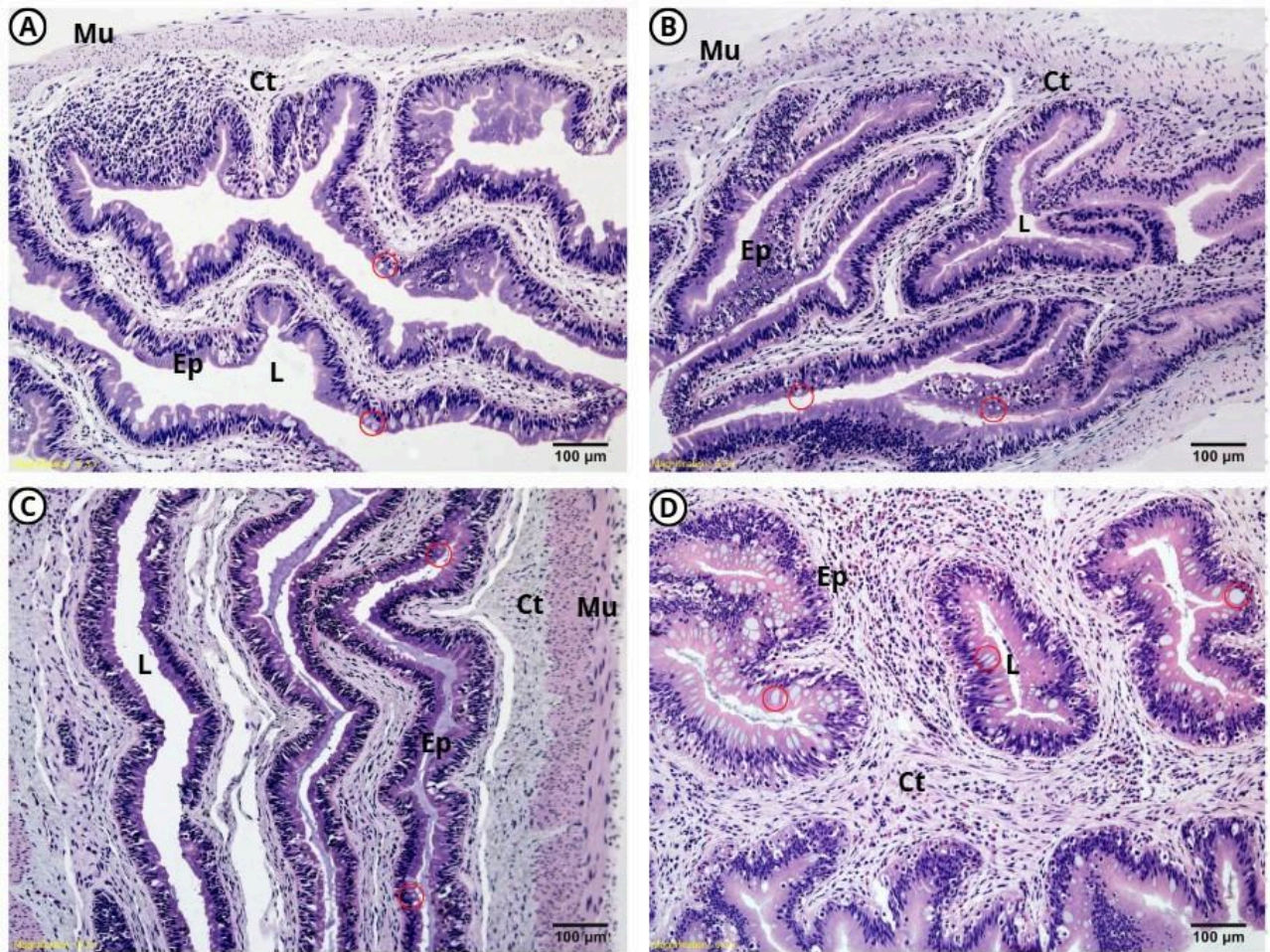


Figure 17. Light microscopy of the intestine of bullfrog (10–20 g) from Group 1 (control), showing no evident lesions. A) Duodenum; B) Jejunum; C) Ileum; and D) Large intestine. All regions exhibit simple columnar epithelium with striated border (Ep) and goblet cells (red circle) in the mucosa, and well-developed connective tissue in the submucosa (Ct). The three segments of the small intestine display a well-defined muscular layer (Mu). The large intestine is organized in crypts. L = lumen.

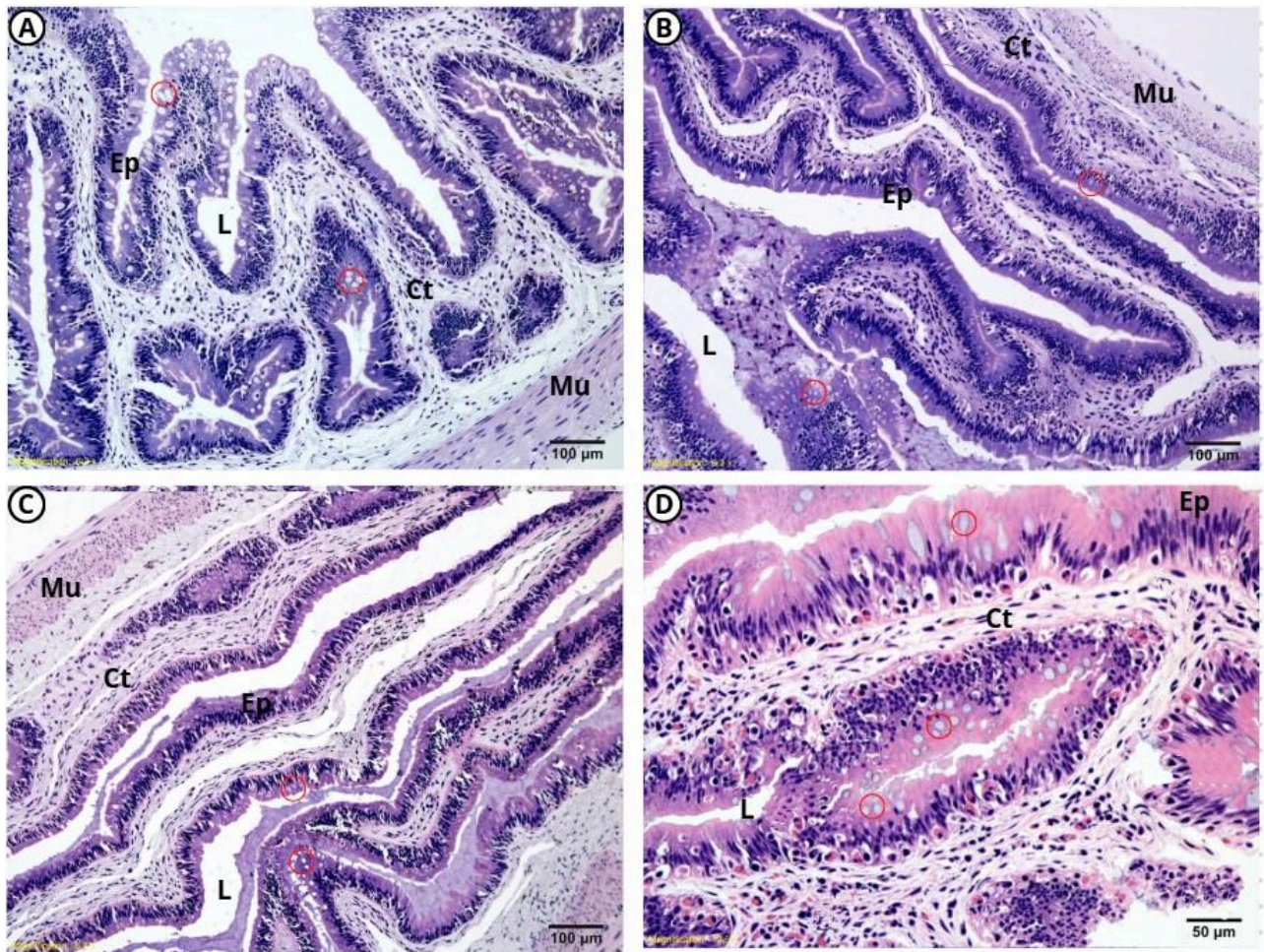


Figure 18. Light microscopy of the intestine of bullfrog (10–20 g) from Group 2 (challenge), showing no evident lesions. A) Duodenum; B) Jejunum; C) Ileum; and D) Large intestine. All regions exhibit simple columnar epithelium with striated border (Ep) and goblet cells (red circle) in the mucosa, and well-developed connective tissue in the submucosa (Ct). The small intestine segments display a well-defined muscular layer (Mu). The large intestine is organized in crypts. L = lumen.

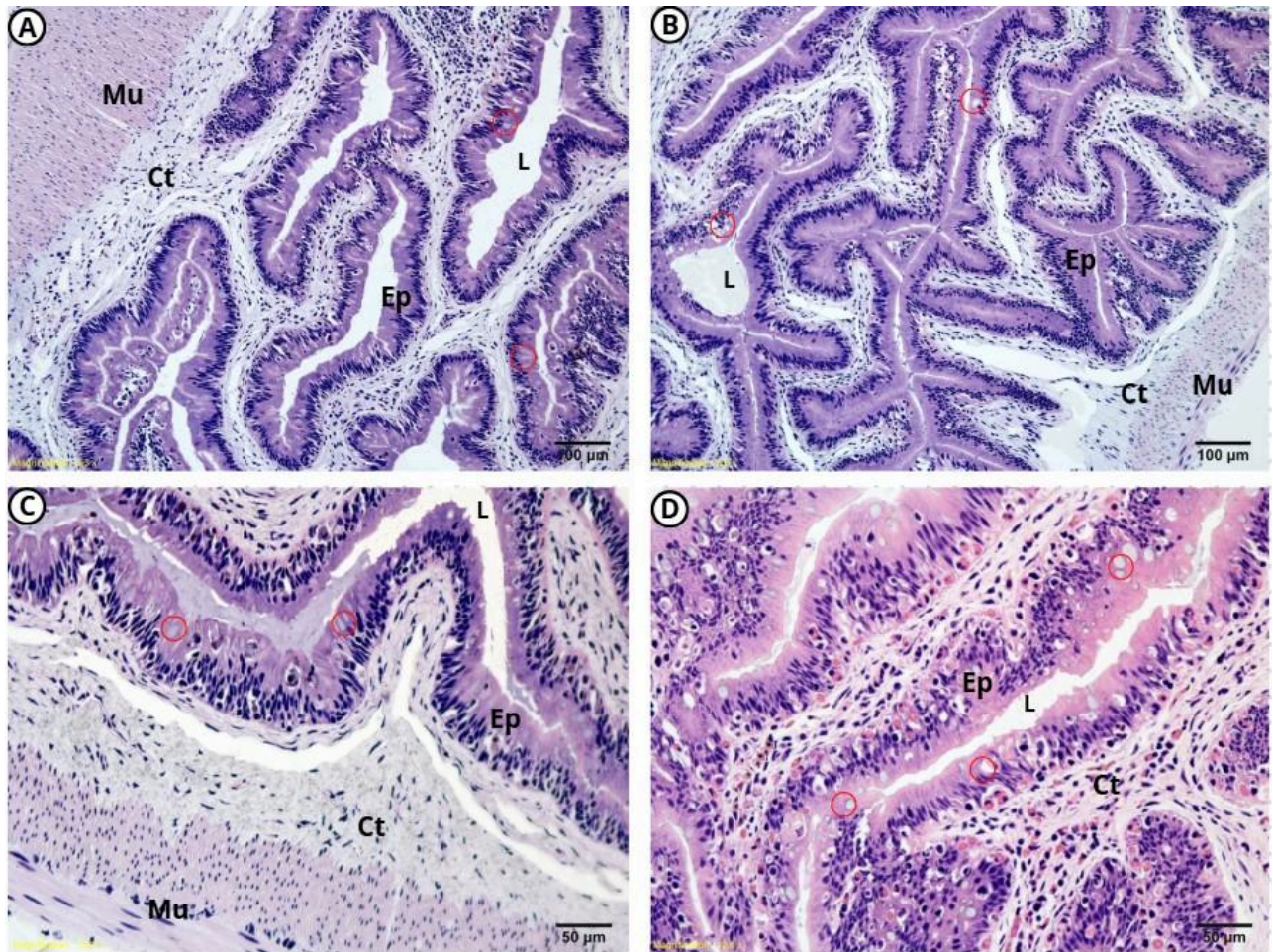


Figure 19. Light microscopy of the intestine of bullfrog (10–20 g) from Group 3 (treatment), showing no evident lesions. A) Duodenum; B) Jejunum; C) Ileum; and D) Large intestine. All regions exhibit simple columnar epithelium with striated border (Ep) and goblet cells (red circle) in the mucosa, and well-developed connective tissue in the submucosa (Ct). The small intestine segments display a well-defined muscular layer (Mu). The large intestine is organized in crypts. L = lumen.

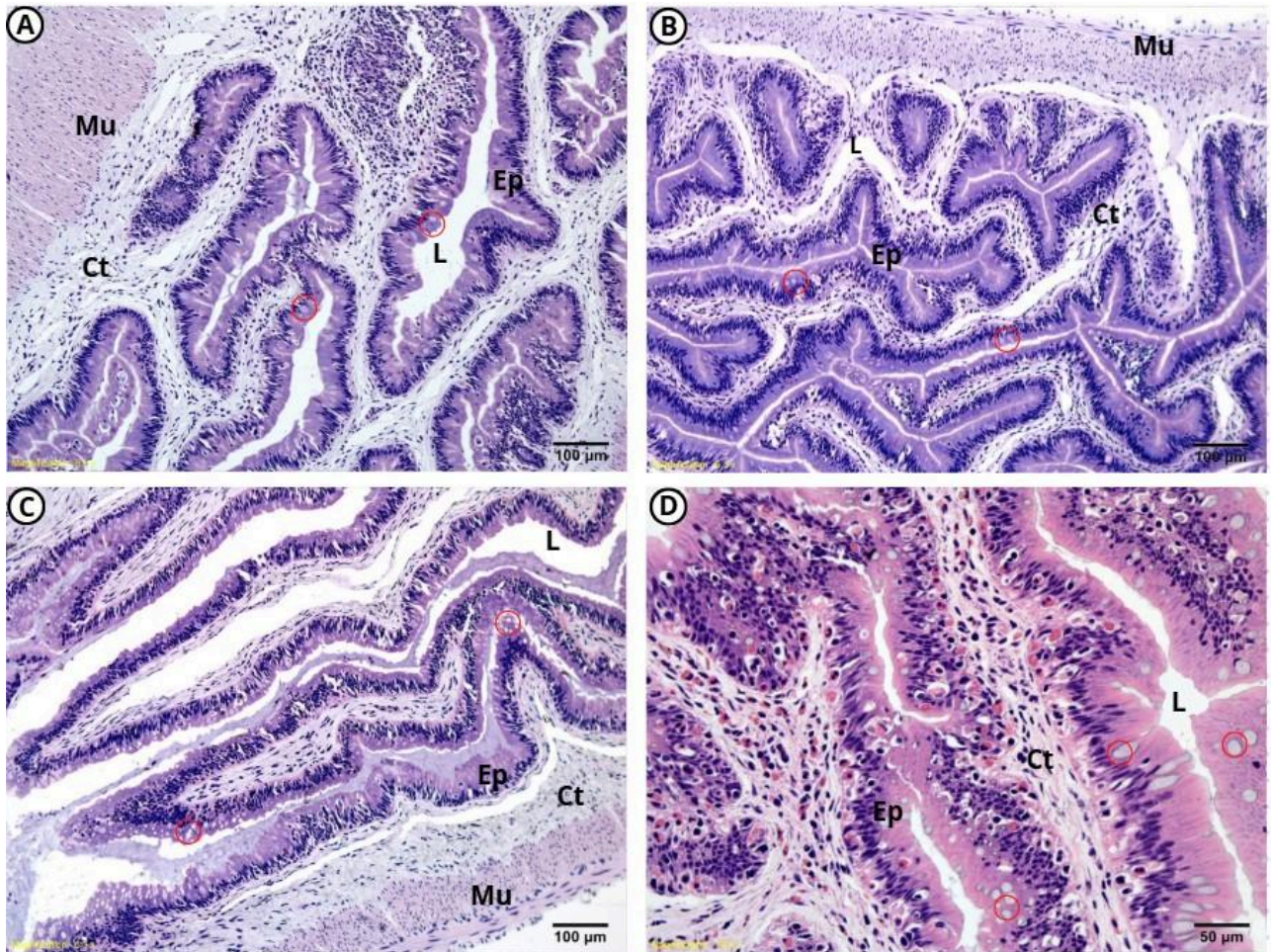


Figure 20. Light microscopy of the intestine of bullfrog (10–20 g) from Group 4 (phage), showing no evident lesions. A) Duodenum; B) Jejunum; C) Ileum; and D) Large intestine. All regions exhibit simple columnar epithelium with striated border (Ep) and goblet cells (red circle) in the mucosa, and well-developed connective tissue in the submucosa (Ct). The three small intestine segments display a well-defined muscular layer (Mu). The large intestine is organized in crypts. L = lumen.

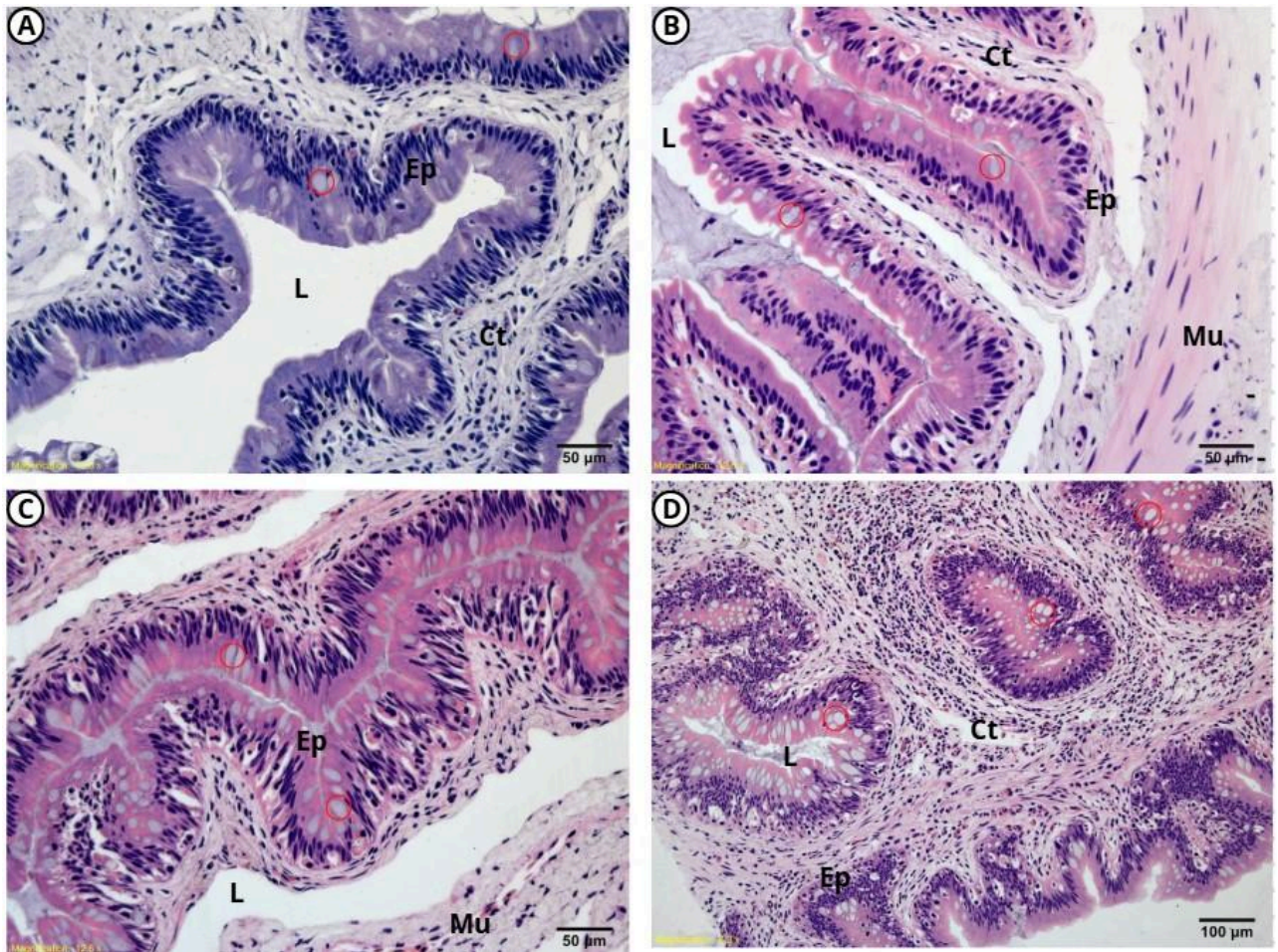


Figure 21. Light microscopy of the intestine of bullfrog (80–100 g) from Group 1 (control), showing no evident lesions. A) Duodenum; B) Jejunum; C) Ileum; and D) Large intestine. All regions exhibit simple columnar epithelium with striated border (Ep) and goblet cells (red circle) in the mucosa, and well-developed connective tissue in the submucosa (Ct). The muscular layer (Mu) is evident in the jejunum and ileum. The large intestine is organized in crypts. L = lumen.

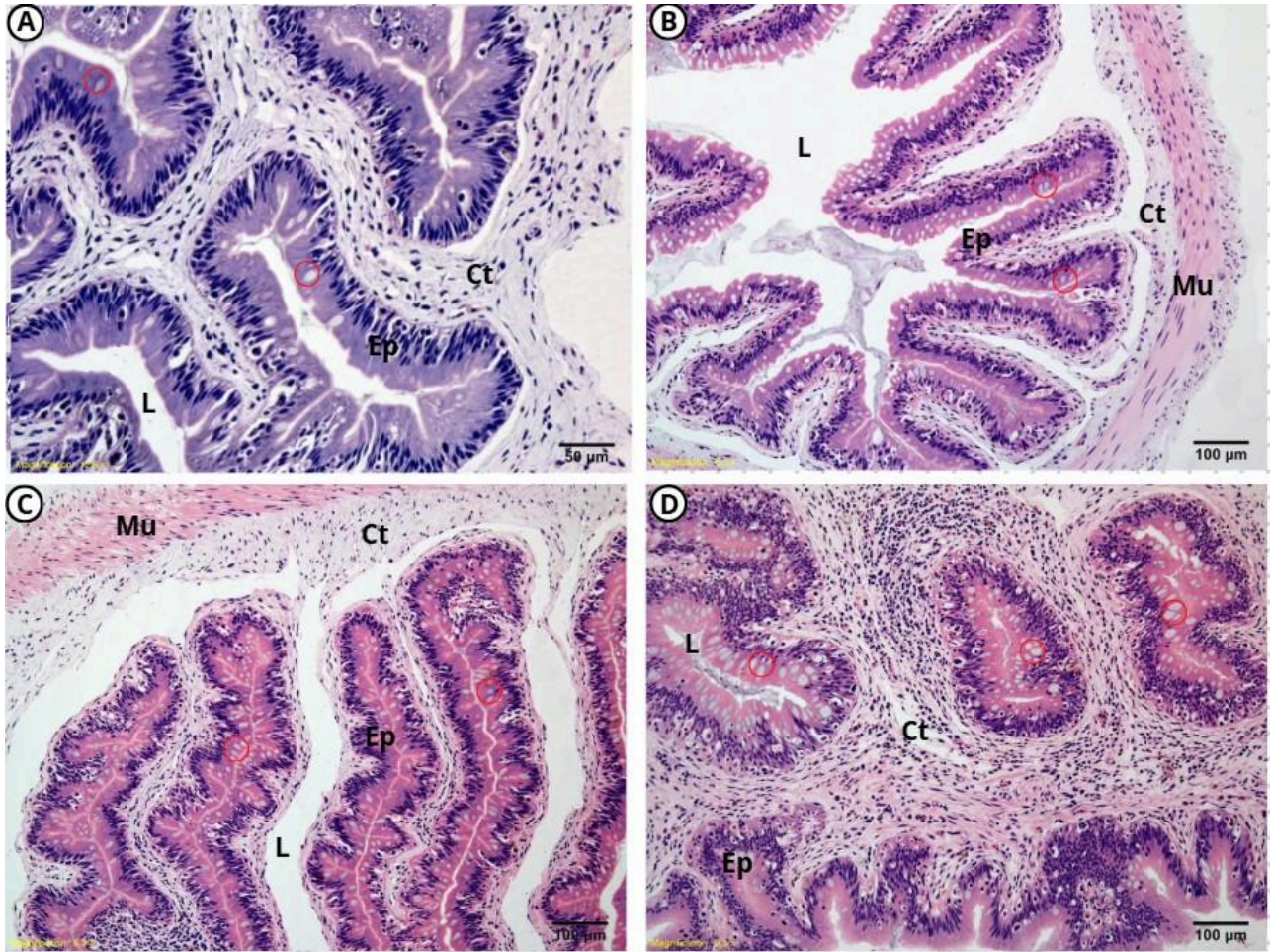


Figure 22. Light microscopy of the intestine of bullfrog (80–100 g) from Group 2 (challenge), showing no evident lesions. A) Duodenum; B) Jejunum; C) Ileum; and D) Large intestine. All regions exhibit simple columnar epithelium with striated border (Ep) and goblet cells (red circle) in the mucosa, and well-developed connective tissue in the submucosa (Ct). The muscular layer (Mu) is evident in the jejunum and ileum. The large intestine is organized in crypts. L = lumen.

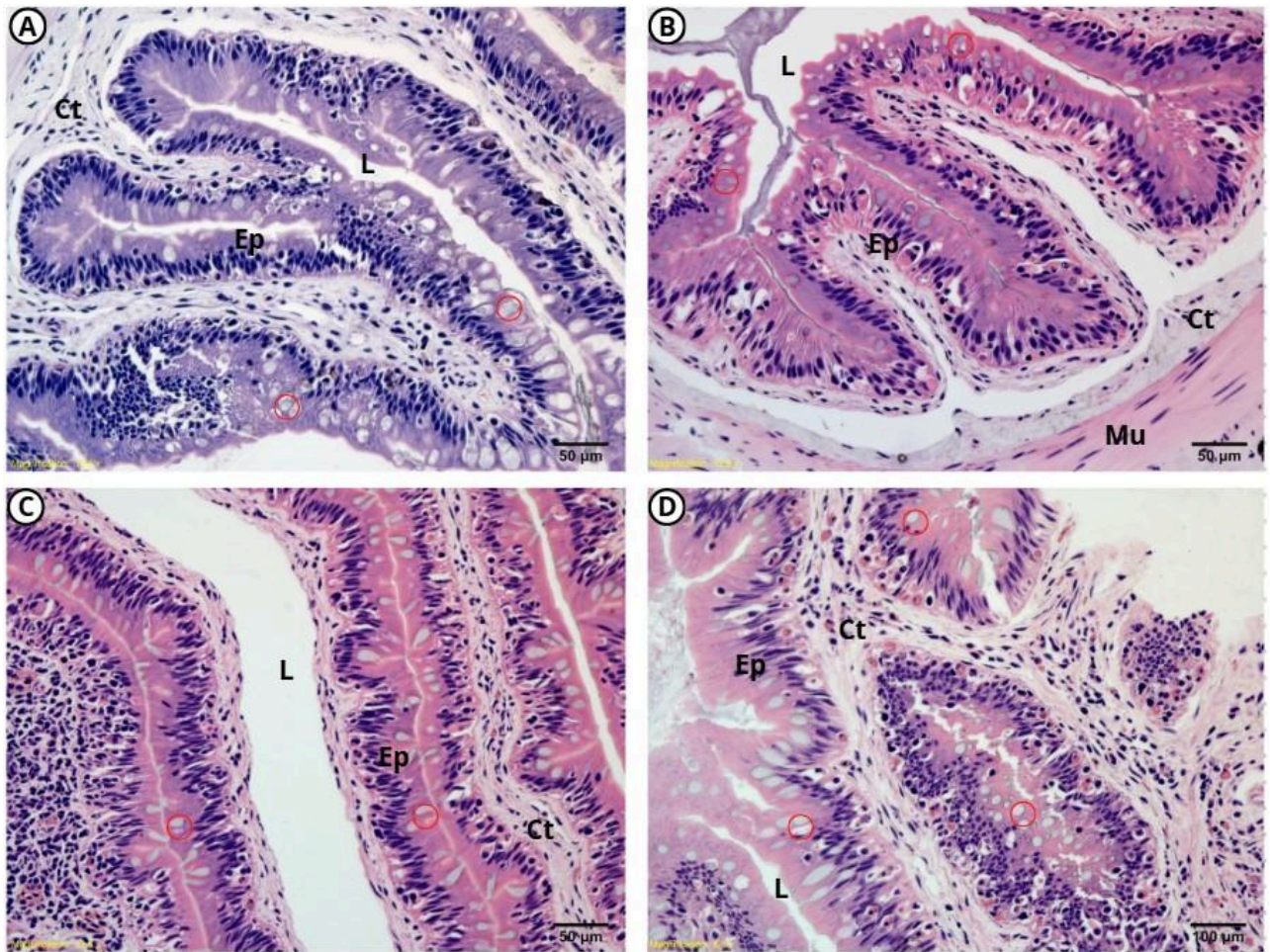


Figure 23. Light microscopy of the intestine of bullfrog (80–100 g) from Group 3 (treatment), showing no evident lesions. A) Duodenum; B) Jejunum; C) Ileum; and D) Large intestine. All regions exhibit simple columnar epithelium with striated border (Ep) and goblet cells (red circle) in the mucosa, and well-developed connective tissue in the submucosa (Ct). The muscular layer (Mu) is evident in the jejunum. The large intestine is organized in crypts. L = lumen.

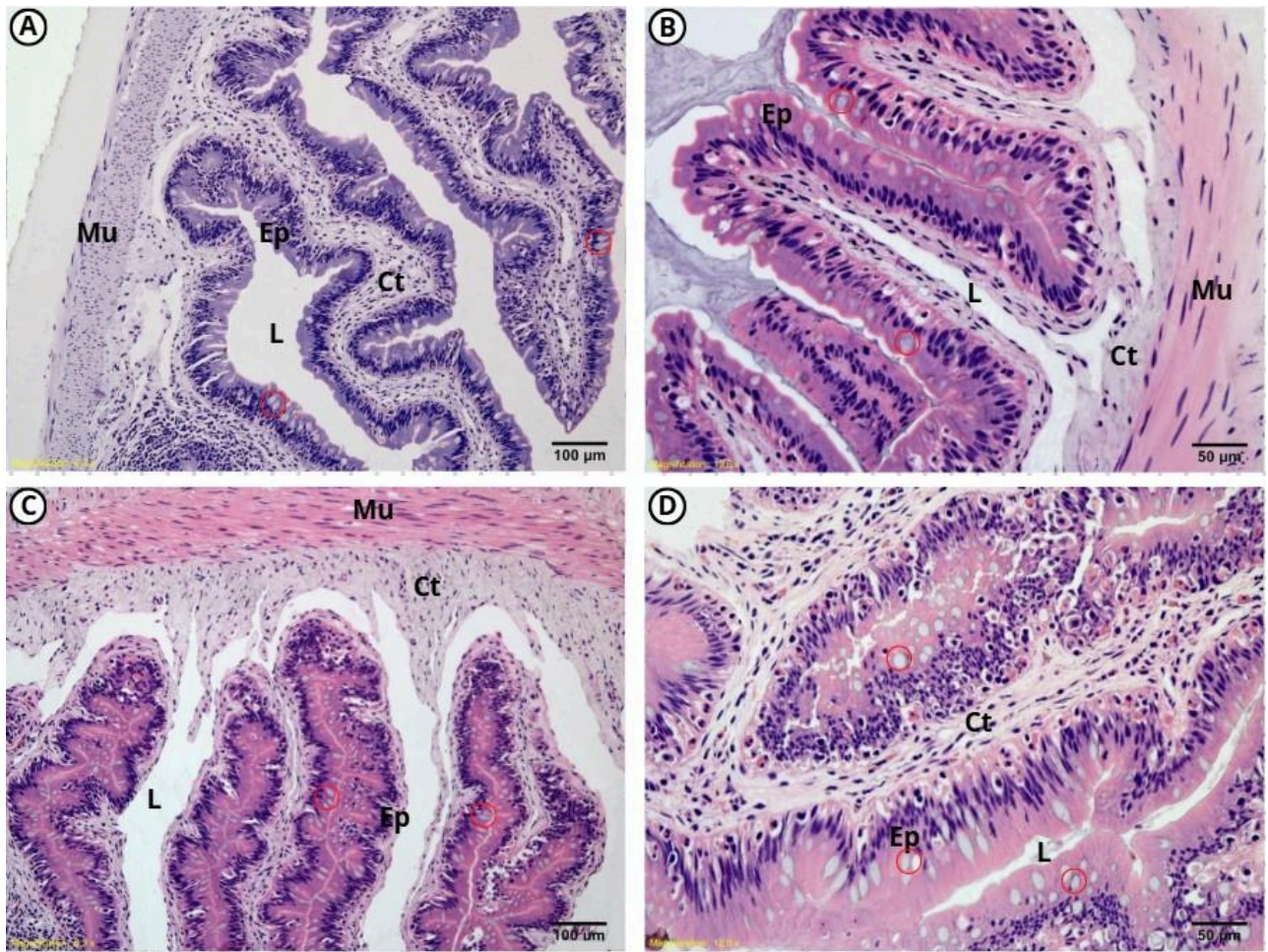


Figure 24. Light microscopy of the intestine of bullfrog (80–100 g) from Group 4 (phage), showing no evident lesions. A) Duodenum; B) Jejunum; C) Ileum; and D) Large intestine. All regions exhibit simple columnar epithelium with striated border (Ep) and goblet cells (red circle) in the mucosa, and well-developed connective tissue in the submucosa (Ct). The three small intestine segments display a well-defined muscular layer (Mu). The large intestine is organized in crypts. L = lumen.

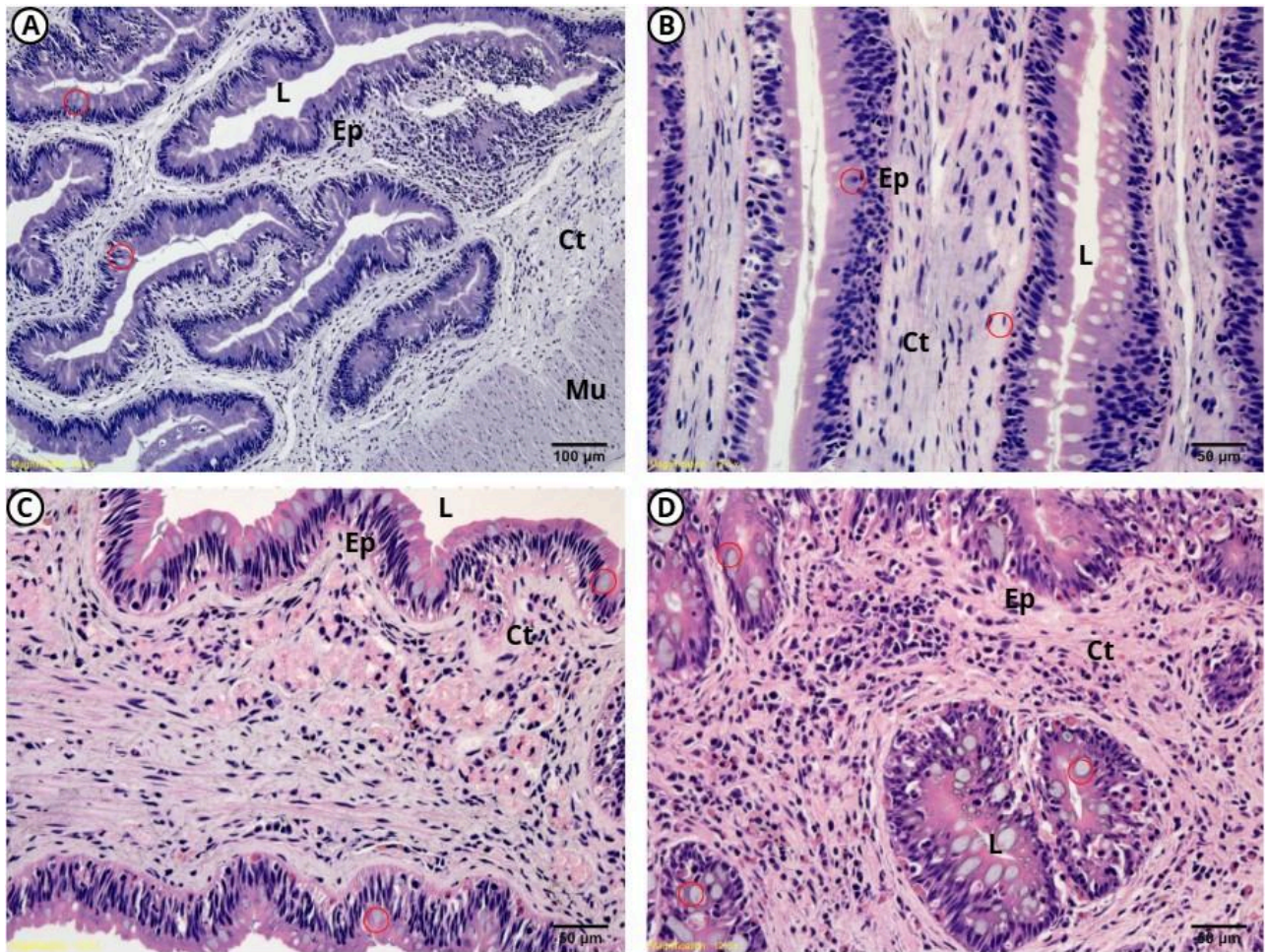


Figure 25. Light microscopy of the intestine of bullfrog (300–350 g) from Group 1 (control), showing no evident lesions. A) Duodenum; B) Jejunum; C) Ileum; and D) Large intestine. All regions exhibit simple columnar epithelium with striated border (Ep) and goblet cells (red circle) in the mucosa, and well-developed connective tissue in the submucosa (Ct). The muscular layer (Mu) is evident in the duodenum. The large intestine is organized in crypts. L = lumen.

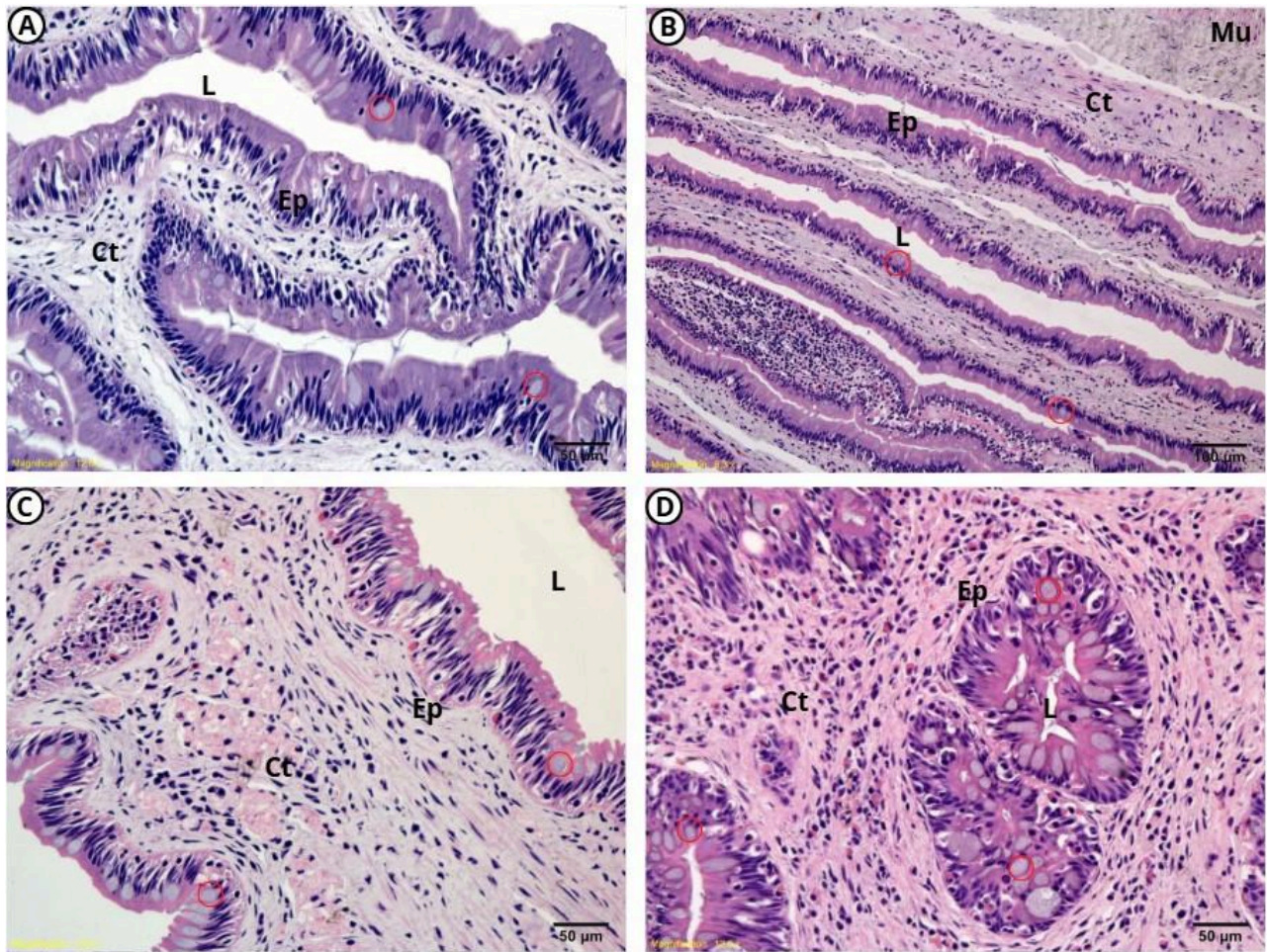


Figure 26. Light microscopy of the intestine of bullfrog (300–350 g) from Group 2 (challenge), showing no evident lesions. A) Duodenum; B) Jejunum; C) Ileum; and D) Large intestine. All regions exhibit simple columnar epithelium with striated border (Ep) and goblet cells (red circle) in the mucosa, and well-developed connective tissue in the submucosa (Ct). The muscular layer (Mu) is evident in the jejunum. The large intestine is organized in crypts. L = lumen.

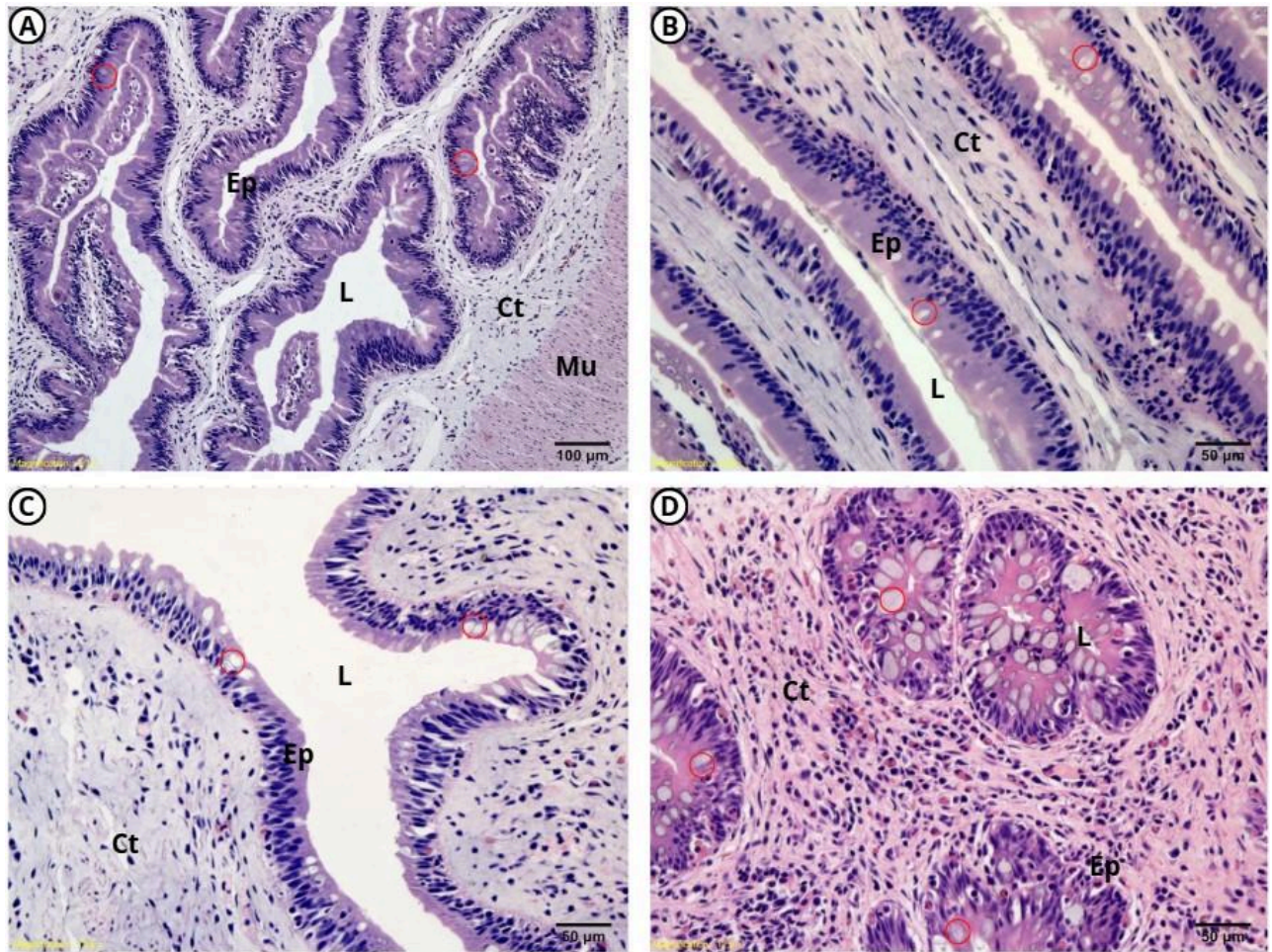


Figure 27. Light microscopy of the intestine of bullfrog (300–350 g) from Group 3 (treatment), showing no evident lesions. A) Duodenum; B) Jejunum; C) Ileum; and D) Large intestine. All regions exhibit simple columnar epithelium with striated border (Ep) and goblet cells (red circle) in the mucosa, and well-developed connective tissue in the submucosa (Ct). The muscular layer (Mu) is evident in the duodenum. The large intestine is organized in crypts. L = lumen.

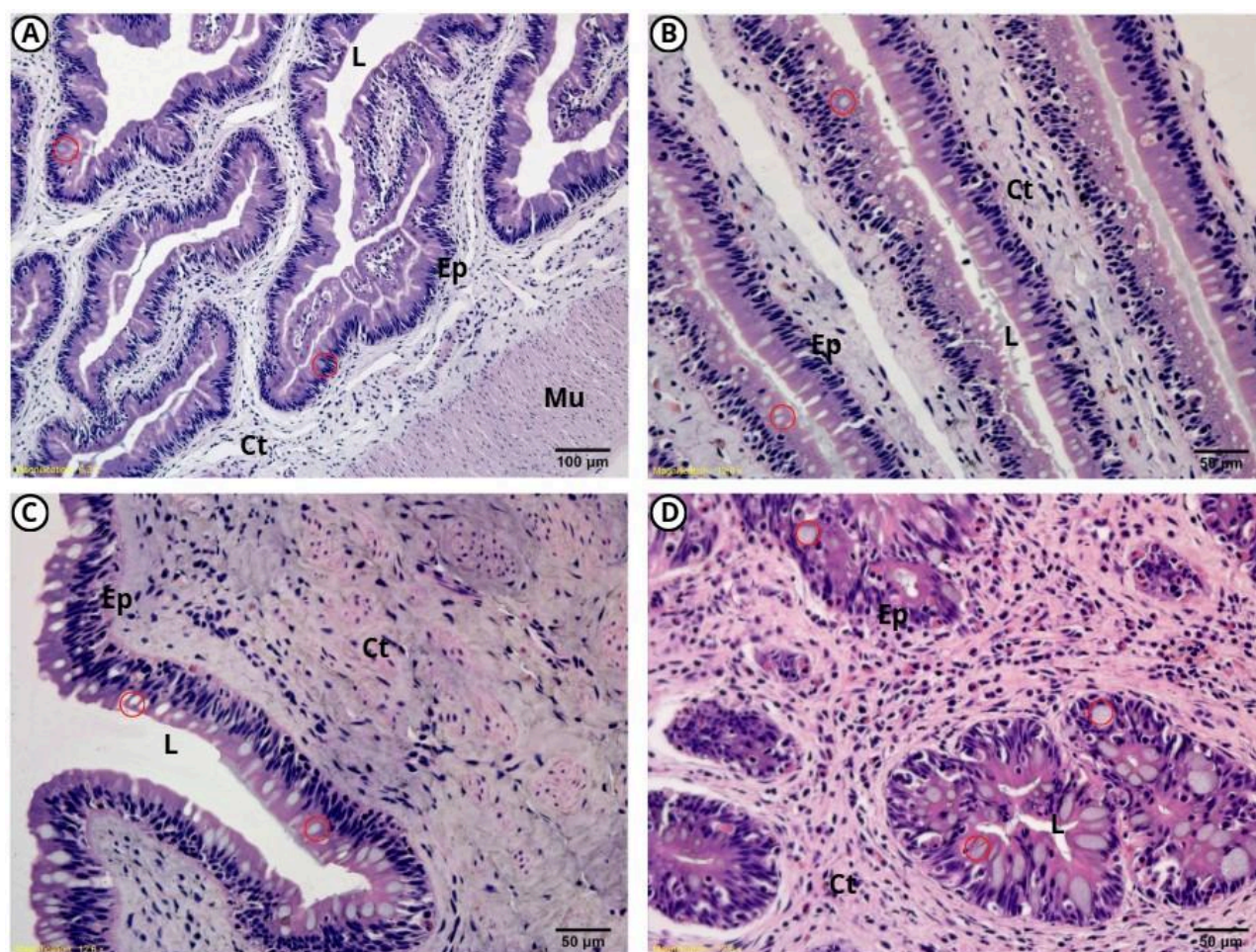


Figure 28. Light microscopy of the intestine of bullfrog (300–350 g) from Group 4 (phage), showing no evident lesions. All regions exhibit simple columnar epithelium with striated border (Ep) and goblet cells (red circle) in the mucosa, and well-developed connective tissue in the submucosa (Ct). The muscular layer (Mu) is evident in the duodenum. The large intestine is organized in crypts. L = lumen.

4.12. Genome analysis

The genome of phage UFVSen15 consists of 156,795 bp of DNA with a GC content of 44.58% and exhibits a 97.26% probability of following a lytic life cycle. No virulence factors or antibiotic resistance genes were detected within the phage genome. Four tRNAs were identified, coding for Methionine, Tryptophan, Asparagine, and Serine. Based on genome annotation, a circular genomic map was generated using Proksee (Figure 29), illustrating gene organization and the distribution of predicted CDSs throughout the genome.

The map highlights the modular arrangement of genes related to replication, virion structure, and bacterial lysis. The circular representation allows clearer visualization of the genomic architecture.

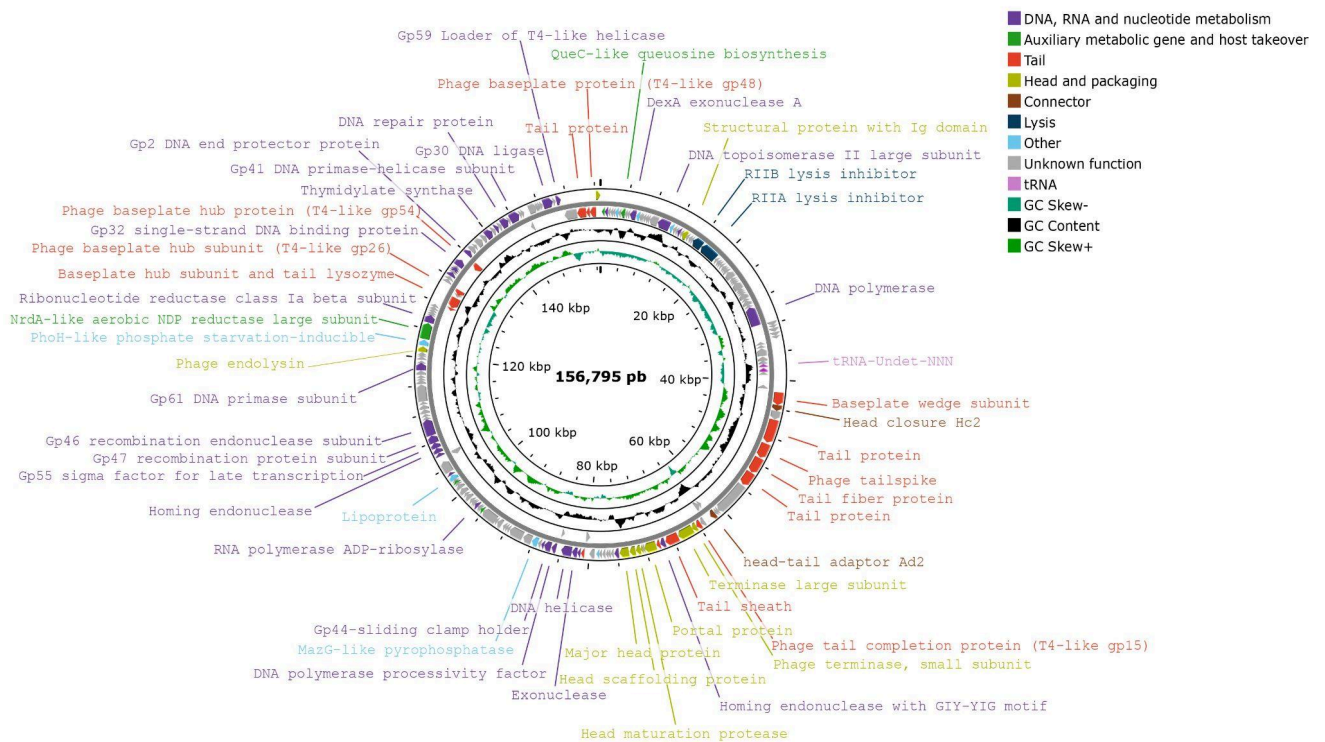


Figure 29. Circular genomic map of phage UFVSen15 generated in Proksee based on functional annotation performed by RAST. Genes encoding hypothetical proteins of unknown function are shown in gray, while other genes are colored according to their predicted functional module.

4.13. Taxonomic assessment and phylogenetics

A search for related phages using BLASTn revealed that the UFVSen15 genome shares high sequence identity with phages deposited in GenBank belonging to the genus *Kuttervirus* (family Ackermannviridae), such as Salmonella phage SenALZ1 (coverage 90%; identity 96%; accession number NC_049440.1), Salmonella phage SeSz-1 (coverage 90%; identity 97%; accession number NC_049443.1), and Salmonella phage SP1 (coverage 90%;

identity 96%; accession number NC_049396.1). This phylogenetic relationship was supported by genome-based phylogenetic reconstruction (Figure 30), where UFVSen15 clustered within a highly conserved monophyletic clade of *Kuttervirus* phages.

Intergenomic similarity analysis using VIRIDIC (Figure 31) quantified genomic proximity. UFVSen15 exhibited similarity scores above 80% with several representatives of the genus, notably Salmonella phage SenALZ1 (88%), Salmonella phage PhiSH19 (87%), and Salmonella phage SeSz-1 (86.7%). Considering that the International Committee on Taxonomy of Viruses (ICTV) defines a 95% genome identity threshold for species delineation, and that the highest score obtained for UFVSen15 was 88%, the data support that this phage represents a new species within the genus *Kuttervirus*.

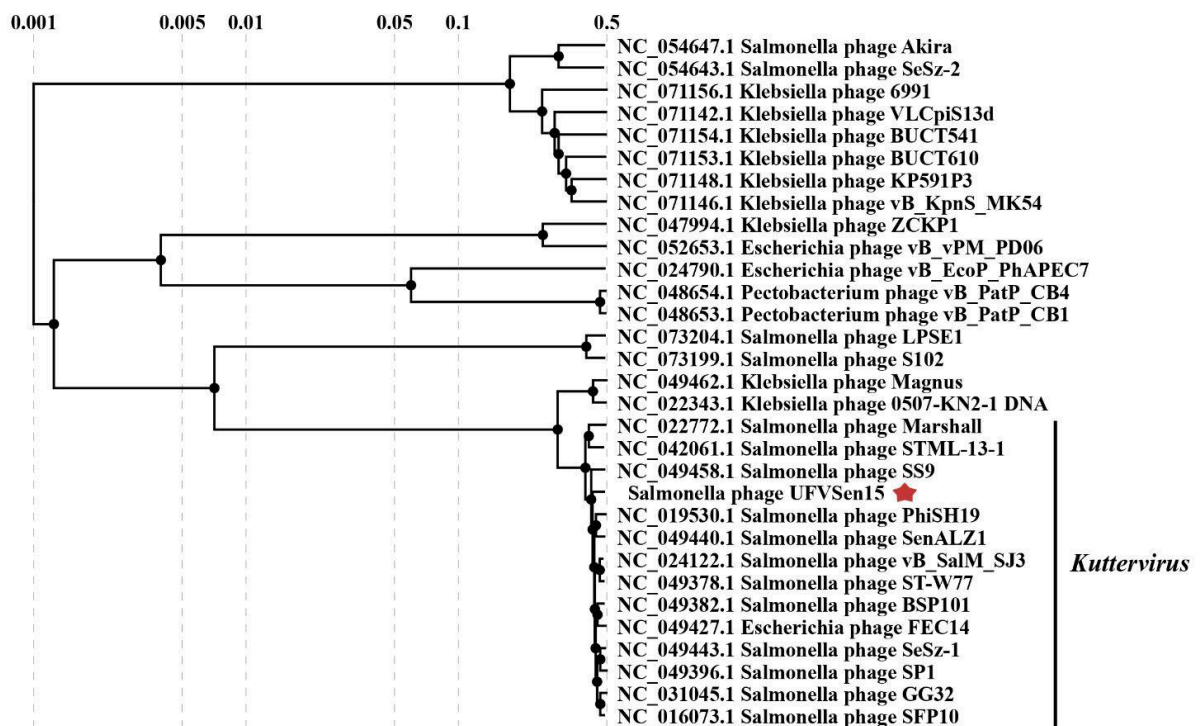


Figure 30. Proteomic tree of phage UFVSen15 (red star) generated by the VipTree web software, showing the phage clustered with representatives of the family Ackermannviridae.

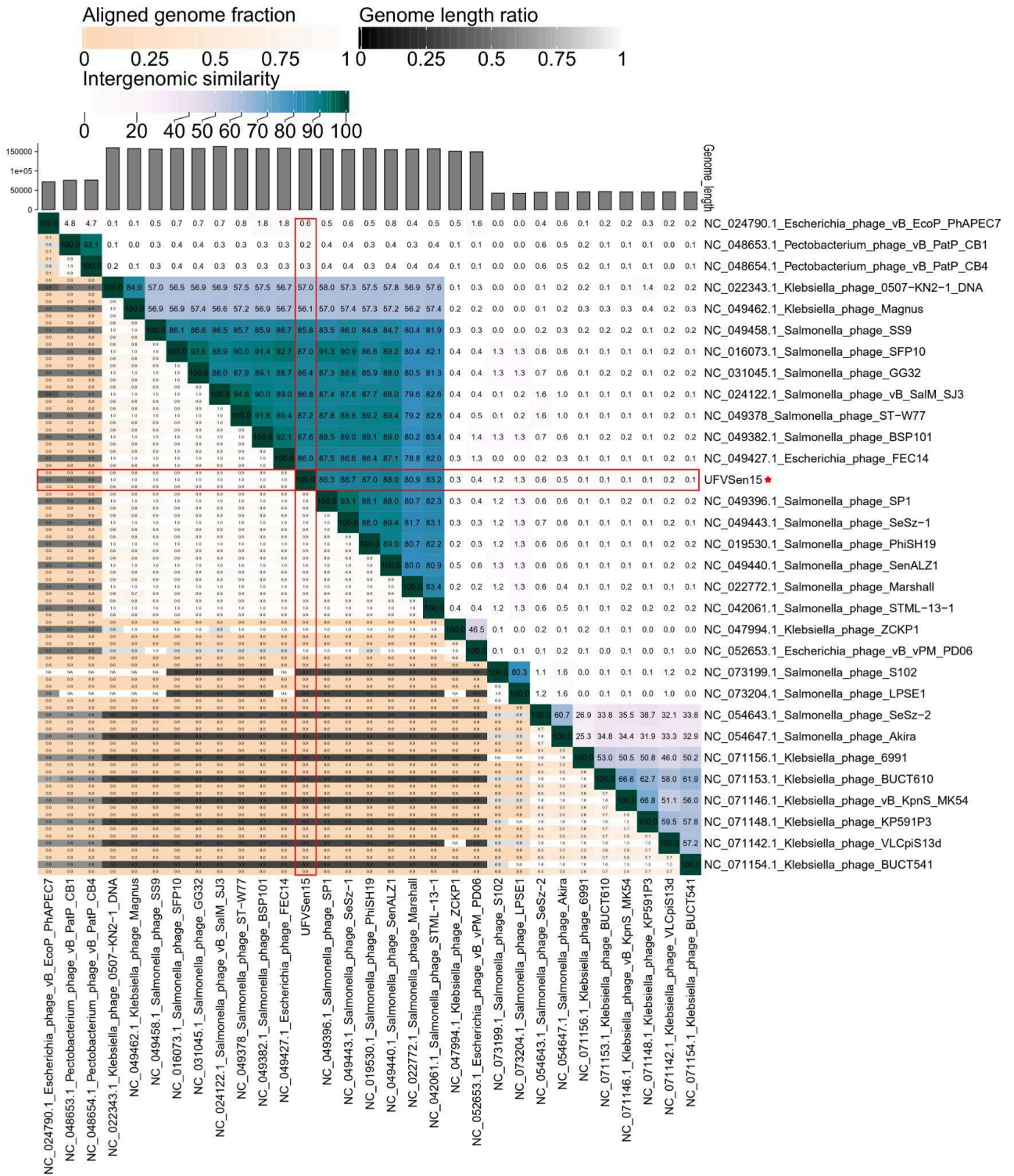


Figure 31. Intergenomic distance map generated by VIRIDIC, illustrating relationships among related phages. Phages with >95% similarity belong to the same species, while those with >70% similarity belong to the same genus.

5. DISCUSSION

The use of phage cocktails, rather than individual phages, is widely advocated in the literature as a key strategy to mitigate the emergence of resistant bacterial variants and to broaden the lytic spectrum against the diversity of *Salmonella* serovars (Islam et al., 2021; Aguilera et al., 2022).

The present study described the isolation and molecular and biological characterization of the bacteriophages UFVSen15 and UFVSmin65, aiming to prospect lytic agents for the biological control of *Salmonella enterica*. The selection of these isolates, integrated with the phage previously characterized by Cunha (2025), was based on the strategic need to compose a trivalent phage cocktail with potential application both *in vitro* and *in vivo*.

The phages UFVSen15 and UFVSmin65 were recovered in the city of Viçosa, Minas Gerais, Brazil, from domestic wastewater and poultry litter, respectively. The recovery of phage isolates from these matrices is consistent with the literature, which identifies such environments as reservoirs rich in *Salmonella* hosts (Ballesté et al., 2022; Unverdi et al., 2024). The presence of viable phages in these samples reflects the local ecology, where the constant selective pressure between viruses and bacteria in high-organic-load niches favors the isolation of novel lytic agents with biotechnological potential (Wiggins & Alexander, 1985; Dion et al., 2020).

In this context, the biological characterization of these new isolates represents a fundamental step to validate their applicability in the control of *Salmonella*. Host range analysis demonstrated the polyvalent nature of the bacteriophages UFVSen15 and UFVSmin65, both capable of lysing multiple *Salmonella enterica* serovars, in agreement with recent findings reported by Arista-Regalado et al. (2024). However, compared to the study by Esmael et al. (2021), the phages characterized here exhibited a broader lytic spectrum, as in that work, activity was limited to only four serovars (Typhimurium, Enteritidis, Typhi, and

Kentucky). This expanded host range may reflect differences in the bacterial receptors recognized by the phages or their adaptability to structural variations among serovars. From an epidemiological perspective, this feature is particularly relevant, considering the high diversity of serovars associated with foodborne outbreaks and infections in various hosts (Spricigo et al., 2013; Fong et al., 2021).

Conversely, the isolated phages did not exhibit lytic activity against other Gram-negative bacteria, such as *Citrobacter freundii* ATCC 8090 and *Shigella flexneri* 12022, nor against the Gram-positive bacterium *Staphylococcus aureus* 046. This result demonstrates the high specificity of the phages for *S. enterica*, a trait widely described for bacteriophages and considered advantageous from a therapeutic standpoint. Unlike broad-spectrum antimicrobials, phages tend to preserve non-target microbiota, reducing undesired ecological impacts and the risk of dysbiosis (Loc-Carrillo & Abedon, 2011).

Notably, both bacteriophages exhibited higher Efficiency of Plating (EOP) values on *S. Enteritidis* (2.33 and 1.14, respectively) compared to their original host strains. This phenomenon suggests a high adsorption affinity or greater compatibility with the replicative machinery of this strain, positioning these phages as strategic candidates for the biological control of *S. Enteritidis*, one of the main pathogens in the poultry, food, and aquaculture production chains (Sillankorva et al., 2012; Chambers & Hulse, 2006; Gantois et al., 2009).

The ability of the UFVSen15 and UFVSmin65 isolates to recognize and lyse different *Salmonella* serovars can be correlated with their morphological features revealed by Transmission Electron Microscopy. The classification of both phages within the class *Caudoviricetes* is based on the presence of a complex tail, a diagnostic structure of this group that is essential for host recognition and the injection of genetic material into Gram-negative bacteria (Switt et al., 2015).

Both UFVSen15 and UFVSmin65 were morphologically classified as myoviruses due to the presence of a long tail equipped with a contractile sheath. This pattern is characteristic of phages possessing a robust structural apparatus composed of multiple proteins involved in the formation of the contractile sheath, a mechanism that perforates the bacterial cell wall and facilitates the injection of viral DNA into the cytoplasm (Fokine & Rossmann, 2014). The presence of this contractile system is frequently associated with higher infection efficiency and, in some cases, a broader host range (Fokine & Rossmann, 2014).

The genomic analysis of UFVSen15 reinforced its taxonomic position, with a genome of 156.8 kb and 88% intergenomic similarity with phages of the genus *Kuttervirus* according to VIRIDIC, below the 95% threshold established by the International Committee on Taxonomy of Viruses for species delineation, suggesting that UFVSen15 represents a new species within this genus. Recent studies highlight the diversity of host recognition domains among phages of the *Ackermannviridae* family (including *Kuttervirus*), which have potential to be used as biocontrol agents against various *Salmonella* strains (Guenther et al., 2012; Switt et al., 2015; Nováček et al., 2016; Mahmoud et al., 2018).

Furthermore, the computational prediction of a lytic cycle for UFVSen15 (97.26%) and the absence of virulence or antibiotic resistance genes reinforce its potential for biocontrol applications and phage therapy, as the presence of lytic genes and the absence of resistance elements are essential criteria for biological safety. These features allow the use of these agents not only in the sanitization of industrial surfaces and food biopreservation but also in veterinary phage therapy and the decontamination of agro-industrial effluents, mitigating the environmental dissemination of *Salmonella* (Moye et al., 2018; Liu et al., 2022).

UFVSen15 exhibited an intermediate latent period (30 min), longer than the 15 and 25 min observed for phages SPHG3 and SPHG1 (EsmaelAEL et al., 2021), but shorter than that reported for phage vB_StyS-LmqSP1 (60 min) (Shakeri et al., 2021). Although it does not

present the shortest latency among the compared phages, it stands out for its high productivity, with a burst size of 254 PFU per cell, considerably higher than the yields reported for SPHG1 and SPHG3. This suggests a replicative strategy oriented toward high viral output per infection cycle, a desirable trait for biocontrol applications.

In contrast, UFVSmin65 showed a latent period of 40 min and a burst size of 19.8 PFU per cell, consistent with lower-productivity phages described in the literature (Abedon, 2009; Hyman & Abedon, 2010; Chen et al., 2024). Although less “explosive,” this profile may be strategically advantageous, as highly productive phages impose strong selective pressure and may accelerate the emergence of resistance (Oechslin, 2018), whereas phages with a more moderate replication dynamic contribute to modulating this pressure. Thus, the contrasting profiles of UFVSen15 and UFVSmin65 support the functional complementarity of the cocktail, combining rapid bacterial reduction with greater evolutionary stability (Chan et al., 2013).

Stability assays of phage UFVSmin65 demonstrated moderate tolerance to pH variations, with complete inactivation at pH 2, but maintenance of titers between pH 3 and 11. The stability observed at pH 3, similar to that reported for UFVSen15, indicates robustness under moderately acidic conditions, surpassing the sensitivity described by Jurczak-Kurek et al. (2016), who reported a significant reduction in viability at pH 4 for other phages. Conversely, the marked decline in titer at pH 12 suggests lower tolerance to highly alkaline environments compared to UFVSen15, possibly due to increased susceptibility of structural proteins to alkaline hydrolysis or surface charge alterations that could compromise virion integrity (Jończyk et al., 2011; Moye et al., 2018).

Regarding thermal stability, UFVSmin65 exhibited greater sensitivity to heat, remaining stable up to 50 °C. A progressive reduction in viability was observed from 60 °C, with complete inactivation at 80 °C and 90 °C, consistent with findings by Jurczak-Kurek et al. (2016) and Phothaworn et al. (2020), who attributed this effect to thermal denaturation of

essential structural proteins, such as tail fibers, compromising host adsorption. Although UFVSmín65 displays a narrower operational thermal range than UFVSen15, it maintains sufficient stability for environmental and aquaculture applications that do not involve exposure to extreme heat, reinforcing its potential as a complementary agent in biocontrol strategies.

Individual MOI assays for each phage demonstrated that UFVSen15 and UFVSmín65 were able to effectively suppress the growth of multiple *Salmonella* serovars, reinforcing their viability as biocontrol agents (Moye et al., 2018). However, the inhibition dynamics varied significantly between the two viral particles. For UFVSen15, a non-linear response was observed, in which a low MOI of 0.01 produced the most pronounced inhibitory effect, suggesting a replication kinetics highly optimized at low MOIs and potential steric interference or premature lysis at higher concentrations (Abedon, 2016). In contrast, UFVSmín65 showed a clear MOI dependence, requiring higher MOIs (MOI 10) to maximize bacterial reduction and maintain a sustained lytic effect throughout the experimental period (Payne & Jansen, 2003). While UFVSen15 was more efficient in delaying the onset of the exponential growth phase, UFVSmín65 stood out for its persistence in bacterial control, particularly against serovars less susceptible to UFVSen15, such as *S. Derby* and *S. Cerro*. The high specificity observed for the genus *Salmonella*, together with the resistant lytic profiles, positions these viruses as excellent candidates for biocontrol strategies, offering broad protection adaptable to different contamination scenarios (Chan et al., 2013).

When evaluating the effect of the phage cocktail at different multiplicities of infection (MOIs), composed of the two phages isolated in this study and the previously described phage Cit2 (Cunha, 2025), high efficiency in controlling *Salmonella* Enteritidis was observed. The analysis demonstrated that the cocktail promoted consistent inhibition of bacterial growth across all tested MOIs, evidencing its effectiveness regardless of the phage:bacteria ratio employed. This prolonged and robust control behavior resembles observations from other studies with polyvalent cocktails, which show greater lytic stability compared to treatments

with individual phages (Hall et al., 2012; Rastegar et al., 2024). Interestingly, at MOIs of 1 and 10, bacterial growth remained suppressed throughout the 24-hour experimental period, highlighting a clear dose-dependent relationship in the intensity and duration of the lytic effect.

This profile partially differs from that observed for the individual phages, which exhibited distinct kinetic behaviors: UFVSen15 demonstrated greater efficiency at low MOIs, whereas UFVSmin65 showed a stronger MOI dependence. Complementarily, the Cit2 phage, previously described by Cunha (2025), also exhibited strong lytic activity against this serovar, although with phases of bacterial regrowth after the initial inhibition when evaluated alone, suggesting limitations in maintaining infectious pressure over time. Bacterial regrowth observed for individual phages is a phenomenon frequently reported in other studies and is generally associated with the selection of resistant mutants or a reduction in infectious pressure over time (Oechslin, 2018; Ambroa et al., 2022).

In this context, the combination of the three phages resulted in a synergistic effect, in which rapid initial suppression and sustained lytic activity prevented bacterial regrowth observed in the individual phage assays (Pereira et al., 2016; Yoo et al., 2023). This effect was also confirmed in solid media, where the cocktail promoted reductions of up to 3 logs in bacterial counts after 24 hours, particularly at higher MOIs. The consistency between these assays reinforces the efficiency and reliability of the cocktail, highlighting its potential for biocontrol applications (Chan et al., 2013; Chen et al., 2018; Chen et al., 2025).

In vivo results in *Aquarana catesbeiana* demonstrated that the phage cocktail significantly reduced *Salmonella* Enteritidis loads, acting both within the host and in the aquatic environment, highlighting an integrated control approach. During the early developmental stage (10–20 g), significant reductions in cloacal colonization and water contamination were observed, with decreases of approximately 1.2 and 1.74 logs, respectively. These findings indicate that the cocktail interfered with the establishment and

persistence of bacterial infection. The higher susceptibility observed in younger animals may be associated with immune immaturity and an intestinal microbiota still undergoing establishment after metamorphosis (Woodhams et al., 2014). Furthermore, the initial stages of frog farming represent a critical sanitary period due to high population density and environmental conditions that favor the dissemination of enterobacteria (Ferreira et al., 2006). Similar outcomes have been reported in other animal production systems, such as poultry, where bacteriophages induced 1–3 log reductions in *Salmonella* loads, demonstrating their efficacy in pathogen control (Atterbury et al., 2007).

The greater bacterial reduction observed in water compared to the intestinal tract indicates that the aquatic environment constitutes the main reservoir of the pathogen in the rearing system (Woo & Bruno, 2011; Costa et al., 2021). In this context, the direct application of bacteriophages to the water reduces the environmental load and interrupts one of the main mechanisms of *Salmonella* maintenance and dissemination in aquaculture systems (Richards, 2014).

In higher weight ranges (80–100 g and 300–350 g), no cloacal colonization by *S. Enteritidis* was detected, suggesting lower susceptibility to intestinal colonization in more developed animals, possibly due to the maturation of the immune system and the establishment of a more stable intestinal microbiota (Kamada et al., 2013; Sommer & Bäckhed, 2013). However, the persistence of the bacteria in the water of the control group demonstrates that the environment can act as a reservoir independently of detectable colonization in the animals.

This aspect is particularly relevant, as amphibians can act as asymptomatic carriers of *Salmonella*, harboring and disseminating the pathogen without displaying apparent clinical signs (Alfani, 2007; Vieira et al., 2014). This silent carriage poses a significant public health risk, as human salmonellosis outbreaks have been associated with contact with contaminated aquatic frogs (CDC, 2010). In this context, the significant reduction of bacterial load in water

promoted by the phage cocktail, reaching up to 2.53 logs, has considerable sanitary relevance.

Thus, decontamination of the aquatic environment directly contributes to reduced cross-contamination and limits the persistence and dissemination of the pathogen within the production system (Defoirdt et al., 2011; Richards, 2014). Consequently, lowering the environmental load reduces the risk of contamination during handling, slaughter, and processing, minimizing the likelihood of pathogen introduction into the food chain and enhancing production safety (Buncic & Sofos, 2012).

The high stability of the phage cocktail in water, with titers maintained around 10^7 PFU/mL, demonstrates its viability under typical frog-farming conditions and its capacity to maintain prolonged activity (Ly-Chatain, 2014). This persistence represents a significant advantage over chemical sanitizers, as it allows continuous pathogen control without generating environmental residues. Therefore, the use of bacteriophages constitutes a promising strategy to strengthen biosecurity programs, reduce environmental contamination, and contribute to the microbiological safety of production, with the potential to decrease reliance on conventional antimicrobials (Sillankorva et al., 2012; Sulakvelidze, 2013).

In addition to the microbiological findings, histological analysis of the bullfrog intestine revealed preservation of the epithelial organization, connective tissue, and muscular layer, as well as the absence of inflammatory infiltrates or degenerative alterations, suggesting that *Salmonella* infection did not trigger adverse tissue responses. The observed morphological pattern was consistent with that described in the literature for amphibians (Duellman & Trueb, 1986; Kardong, 1998), corroborating the maintenance of intestinal architecture within physiologically normal parameters. Furthermore, considering that frogs are recognized asymptomatic carriers of *Salmonella*, the absence of inflammatory changes or histopathological lesions is biologically coherent (Alfani, 2007; Vieira et al., 2014). Taken together, these findings indicate that the phage cocktail was effective in controlling the bacterium under the experimental conditions evaluated, without compromising the structural

integrity of the bullfrog intestine, reinforcing its potential as a safe biological strategy.

Additionally, future studies focusing on the complete genomic characterization of phage UFVSmin65 will be essential to elucidate its mechanisms of action and confirm its biological safety and stability, while research in other contexts, such as poultry farming, the food industry, and industrial environments, could evaluate the efficacy and applicability of the phage cocktail under different scenarios. Taken together, these results demonstrate that the phage cocktail exhibited high efficacy in reducing *Salmonella* Enteritidis under both *in vitro* and *in vivo* conditions, coupled with high specificity, enabling a targeted action against the pathogen without interfering with the beneficial microbiota. These findings reinforce the potential of bacteriophages as promising agents for the biocontrol of *Salmonella enterica* in aquaculture systems.

6. CONCLUSIONS

This study enabled the biological characterization of bacteriophages UFVSen15 and UFVSmin65, as well as the genomic characterization of UFVSen15, highlighting its potential as a biocontrol agent against *Salmonella enterica*. Both phages exhibited a host range targeting relevant serovars, demonstrating high lytic specificity. In addition, they showed stability across a wide range of pH and temperatures, along with efficient replication, with growth parameters compatible with biotechnological applications and large-scale production. The phage cocktail composed of these isolates together with phage UFVCit2 demonstrated high efficacy in inhibiting *Salmonella* Enteritidis, achieving significant reductions in bacterial populations under both *in vitro* and *in vivo* conditions. These results reinforce the potential of bacteriophages as a safe, specific, and sustainable strategy for controlling this pathogen. Overall, the findings of this study contribute to advancing the knowledge on the use of bacteriophages as a promising alternative for controlling *Salmonella enterica*, particularly in aquaculture systems, representing an innovative approach for managing bacterial infections and reducing the use of antimicrobials.

REFERENCES

- Abd El-Ghany WA. Salmonellosis: A food borne zoonotic and public health disease in Egypt. *J Infect Dev Ctries*. 2020 Jul 31;14(7):674–678. doi:10.3855/jidc.12739.
- Abedon ST. Kinetics of phage-mediated biocontrol of bacteria. *Foodborne Pathog Dis*. 2009;6(7):807–815. doi:10.1089/fpd.2008.0242.
- Abedon ST. Phage therapy dosing: the problem(s) with multiplicity of infection (MOI). *Bacteriophage*. 2016;6(3):e1220348. doi:10.1080/21597081.2016.1220348.
- Abedon ST, Kuhl SJ, Blasdel BG, Kutter EM. Phage treatment of human infections. *Bacteriophage*. 2011 Mar;1(2):66–85. doi:10.4161/bact.1.2.15845.
- Ackermann HW. Bacteriophage observations and evolution. *Res Microbiol*. 2003 May;154(4):245–251. doi:10.1016/S0923-2508(03)00067-6.
- Ackermann HW. Tailed bacteriophages: the order caudovirales. *Adv Virus Res*. 1998;51:135–201. doi:10.1016/s0065-3527(08)60785-x.
- Ackermann HW, DuBow M. Viruses of prokaryotes I: General properties of bacteriophages. In: *Practical Applications of Bacteriophages*. Boca Raton: CRC Press; 1987.
- Aguilera M, Martínez S, Tello M, Gallardo MJ, García V. Use of cocktail of bacteriophage for *Salmonella Typhimurium* control in chicken meat. *Foods*. 2022;11(8):1164. doi:10.3390/foods11081164.
- Ahmad S, Ahmad M, Khan S, Ahmad F, Nawaz S, Khan FU. An overview on phase variation, mechanisms and roles in bacterial adaptation. *J Pak Med Assoc*. 2017 Feb;67(2):285–291.

Akiba M, Kusumoto M, Iwata T. Rapid identification of *Salmonella enterica* serovars Typhimurium, Choleraesuis, Infantis, Hadar, Enteritidis, Dublin and Gallinarum by multiplex PCR. *J Microbiol Methods*. 2011 Apr;85(1):9–15. doi:10.1016/j.mimet.2011.02.002.

Albarella D, Dall'Ara P, Rossi L, et al. Bacteriophage therapy in freshwater and saltwater aquaculture species. *Microorganisms*. 2025;13(4):831. doi:10.3390/microorganisms13040831.

Alfani R. Ocorrência de *Salmonella* spp. em carcaças e vísceras de rãs (*Rana catesbeiana*) [dissertação]. Botucatu: Faculdade de Medicina Veterinária e Zootecnia, Universidade Estadual Paulista; 2007.

Alomari MMM, Dec M, Urban-Chmiel R. Bacteriophages as an alternative method for control of zoonotic and foodborne pathogens. *Viruses*. 2021;13(12):2348. doi:10.3390/v13122348.

Arrach N, Porwollik S, Cheng P, Cho A, Long F, Choi SH, McClelland M. *Salmonella* serovar identification using PCR-based detection of gene presence and absence. *J Clin Microbiol*. 2008 Aug;46(8):2581–2589. doi:10.1128/JCM.02147-07.

Arista-Regalado AD, Viera-Segura O, de Oca SA, Hernández-Hernández L, González-Aguilar DG, León JB. Characterization and efficacy of *Salmonella* phage cocktail PHA46 in the control of *Salmonella* Newport and Typhimurium internalized into cherry tomatoes. *Int J Food Microbiol*. 2024 Jul 16;419:110745. doi:10.1016/j.ijfoodmicro.2024.110745.

Atterbury RJ, Connerton PL, Dodd CE, Rees CE, Connerton IF. Application of host-specific bacteriophages to the surface of chicken skin leads to a reduction in recovery of *Campylobacter jejuni*. *Appl Environ Microbiol*. 2003 Oct;69(10):6302–6306. doi:10.1128/AEM.69.10.6302-6306.2003.

Atterbury RJ, Van Bergen MA, Ortiz F, Lovell MA, Harris JA, De Boer A, Wagenaar JA, Allen VM, Barrow PA. Bacteriophage therapy to reduce *Salmonella* colonization of broiler chickens. *Appl Environ Microbiol*. 2007;73(14):4543–4549. doi:10.1128/AEM.00049-07.

Ballesté E, Blanch AR, Muniesa M, García-Aljaro C, Rodríguez-Rubio L, Martín-Díaz J, Pascual-Benito M, Jofre J. Bacteriophages in sewage: abundance, roles, and applications. *FEMS Microbes*. 2022 Mar 17;3:xtac009. doi:10.1093/femsmc/xtac009.

Boucher D, Barnich N. Phage therapy against adherent-invasive *E. coli*: towards a promising treatment of Crohn's disease patients? *J Crohns Colitis*. 2022 Nov 1;16(10):1509–1510. doi:10.1093/ecco-jcc/jjac070.

Buncic S, Sofos J. Interventions to control *Salmonella* contamination during poultry, cattle and pig slaughter. In: Sofos J, editor. *Improving the safety of fresh meat*. Cambridge: Woodhead Publishing; 2012. p. 120–156.

Bruce HL, Barrow PA, Rycroft AN. Zoonotic potential of *Salmonella enterica* carried by pet tortoises. *Vet Rec*. 2018 Feb 3;182(5):141. doi:10.1136/vr.104457.

Bumstead N, Barrow P. Resistance to *Salmonella gallinarum*, *S. pullorum*, and *S. enteritidis* in inbred lines of chickens. *Avian Dis*. 1993 Jan–Mar;37(1):189–193.

Cantlay JC, Ingram DJ, Meredith AL. A review of zoonotic infection risks associated with the wild meat trade in Malaysia. *EcoHealth*. 2017;14(3):361–388. doi:10.1007/s10393-017-1229-x.

Carvalho ML, Espindola CS, Nascimento CB, Santos PB. Phage therapy: the use of bacteriophages as an alternative for the treatment of antibiotic-resistant bacterial infections. *Rev Ibero-Am Humanid Cienc Educ*. 2024;10(11):1442–1452. doi:10.51891/rease.v10i11.16566.

Centers for Disease Control and Prevention (CDC). Multistate outbreak of human *Salmonella* Typhimurium infections associated with aquatic frogs—United States, 2009–2010. *MMWR Morb Mortal Wkly Rep*. 2010;59(1):1–5.

Chambers DL, Hulse AC. *Salmonella* serovars in the herpetofauna of Indiana County, Pennsylvania. *Appl Environ Microbiol*. 2006 May;72(5):3771–3773. doi:10.1128/AEM.72.5.3771-3773.2006.

Chan BK, Abedon ST, Loc-Carrillo C. Phage cocktails and the future of phage therapy. *Future Microbiol.* 2013;8(6):769–783. doi:10.2217/fmb.13.47.

Chen CY, Chen WC, Chin SC, Lai YH, Tung KC, Chiou CS, Hsu YM, Chang CC. Prevalence and antimicrobial susceptibility of salmonellae isolates from reptiles in Taiwan. *J Vet Diagn Invest.* 2010 Jan;22(1):44–50. doi:10.1177/104063871002200107.

Chen M, Yu T, Cao X, Pu J, Wang D, Deng H. Isolation and characterization of *Salmonella enteritidis* bacteriophage Salmp-p7 isolated from slaughterhouse effluent and its application in food. *Arch Microbiol.* 2024 Nov 29;207(1):7. doi:10.1007/s00203-024-04206-x.

Chen Y, Sun E, Song J, Tong Y, Wu B. Three *Salmonella enterica* serovar Enteritidis bacteriophages from the Siphoviridae family are promising candidates for phage therapy. *Can J Microbiol.* 2018 Nov;64(11):865–875. doi:10.1139/cjm-2017-0740.

Chen Y, Wang X, Zhang Q, Zhang Z, Liu Z, Zhao X, Li L, Hu M, Lv Q, Luo Y, Xu X, Petersen B, Cai Y, Sicheritz-Pontén T, Clokie MRJ, Liu Y. ABCD-type phage cocktail targeting distinct LPS receptor sites demonstrates superior efficacy against multidrug-resistant *Salmonella*. *J Hazard Mater.* 2025 Dec 5;500:140435. doi:10.1016/j.jhazmat.2025.140435.

Clokie MR, Millard AD, Letarov AV, Heaphy S. Phages in nature. *Bacteriophage.* 2011 Jan;1(1):31–45. doi:10.4161/bact.1.1.14942.

Costa PC, Nascimento YF, Costa LRM, Dias SC, Ventura NKO, Yamatogi RS, Costa FAA, Cossi MVC. Influence of different periods of pre-slaughter fasting on microbiological quality of bullfrog carcasses (*Lithobates catesbeianus*). *Arquivo Brasileiro de Medicina Veterinária e Zootecnia.* 2021;73(2):487–494. doi:10.1590/1678-4162-12030.

Cunha PC, Rodrigues IR, Rosset AJD, Silva JD, Vieira MS, Dias RS, Silva CC, Paula SO. Isolation and characterization of the polyvalent enterobacteria-infecting phage Cit2 with potential

for biocontrol applications. 2025. Doctoral thesis, Universidade Federal de Viçosa, Viçosa, MG, Brazil.

Danis-Wlodarczyk K, Dąbrowska K, Abedon ST. Phage therapy: the pharmacology of antibacterial viruses. *Curr Issues Mol Biol*. 2021;40:81–164. doi:10.21775/cimb.040.081.

Dion MB, Oechslin F, Moineau S. Phage diversity, genomics and phylogeny. *Nat Rev Microbiol*. 2020 Mar;18(3):125–138. doi:10.1038/s41579-019-0311-5.

Duellman WE, Trueb L. *Biology of amphibians*. New York: McGraw-Hill; 1986.

Erez Z, Steinberger-Levy I, Shamir M, Doron S, Stokar-Avihail A, Peleg Y, Melamed S, Leavitt A, Savidor A, Albeck S, Amitai G, Sorek R. Communication between viruses guides lysis-lysogeny decisions. *Nature*. 2017 Jan 26;541(7638):488–493. doi:10.1038/nature21049.

Esmael A, Azab E, Gobouri AA, Nasr-Eldin MA, Moustafa MMA, Mohamed SA, Badr OAM, Abdelatty AM. Isolation and characterization of two lytic bacteriophages infecting a multi-drug resistant *Salmonella* Typhimurium and their efficacy to combat salmonellosis in ready-to-use foods. *Microorganisms*. 2021;9(2):423. doi:10.3390/microorganisms9020423.

Ferreira CM, Rodrigues EB, Sampaio MCP. Criação de rãs (ranicultura). *Inf Agropecu*. 2006;27(235):80–88.

Fong K, Wong CWY, Wang S, Delaquis P. How broad is enough: the host range of bacteriophages and its impact on the agri-food sector. *Phage (New Rochelle)*. 2021 Jun 1;2(2):83–91. doi:10.1089/phage.2020.0036.

Fokine A, Rossmann MG. Molecular architecture of tailed bacterial viruses. *Protein Sci*. 2014;23(7):854–867.

Galán-Relaño Á, Valero Díaz A, Huerta Lorenzo B, Gómez-Gascón L, Mena Rodríguez MÁ, Carrasco Jiménez E, Pérez Rodríguez F, Astorga Márquez RJ. *Salmonella* and salmonellosis: an

update on public health implications and control strategies. *Animals (Basel)*. 2023 Nov 27;13(23):3666. doi:10.3390/ani13233666.

Gantois I, Ducatelle R, Pasmans F, Haesebrouck F, Gast R, Humphrey TJ, Van Immerseel F. Mechanisms of egg contamination by *Salmonella* Enteritidis. *FEMS Microbiol Rev*. 2009 Jul;33(4):718–738. doi:10.1111/j.1574-6976.2008.00161.x.

Gorski L, Jay-Russell MT, Liang AS, Walker S, Bengson Y, Govoni J, Mandrell RE. Diversity of pulsed-field gel electrophoresis pulsotypes, serovars, and antibiotic resistance among *Salmonella* isolates from wild amphibians and reptiles in the California Central Coast. *Foodborne Pathog Dis*. 2013 Jun;10(6):540–548. doi:10.1089/fpd.2012.1372.

Guenther S, Herzig O, Fieseler L, Klumpp J, Loessner MJ. Biocontrol of *Salmonella* Typhimurium in RTE foods with the virulent bacteriophage FO1-Eint. *J Food Microbiol*. 2012;154:66–72.

Guerra B, Helmuth R, Thomas K, Beutlich J, Jahn S, Schroeter A. Plasmid-mediated quinolone resistance determinants in *Salmonella* spp. isolates from reptiles in Germany. *J Antimicrob Chemother*. 2010 Sep;65(9):2043–2045. doi:10.1093/jac/dkq242.

Hall AR, De Vos D, Friman VP, Pirnay JP, Buckling A. Effects of sequential and simultaneous applications of bacteriophages on populations of *Pseudomonas aeruginosa* *in vitro* and in wax moth larvae. *Appl Environ Microbiol*. 2012 Aug;78(16):5646–5652. doi:10.1128/AEM.00757-12.

Hankin ME. The bactericidal action of the waters of the Jamuna and Ganges rivers on cholera microbes. *Ann Inst Pasteur*. 1896;10:511–523.

Havelaar AH, Kirk MD, Torgerson PR, Gibb HJ, Hald T, Lake RJ, Praet N, Bellinger DC, de Silva NR, Gargouri N, Speybroeck N, Cawthorne A, Mathers C, Stein C, Angulo FJ, Devleeschauwer B; WHO Foodborne Disease Burden Epidemiology Reference Group. World Health Organization global estimates and regional comparisons of the burden of foodborne disease in 2010. *PLoS Med*. 2015 Dec 3;12(12):e1001923. doi:10.1371/journal.pmed.1001923.

Herikstad H, Motarjemi Y, Tauxe RV. Salmonella surveillance: a global survey of public health serotyping. *Epidemiol Infect.* 2002 Aug;129(1):1–8. doi:10.1017/s0950268802006842.

Hesse S, Adhya S. Phage therapy in the twenty-first century: facing the decline of the antibiotic era; is it finally time for the age of the phage? *Annu Rev Microbiol.* 2019 Sep 8;73:155–174. doi:10.1146/annurev-micro-090817-062535.

Huang T, Gu D, Guo Y, Li A, Kang X, Jiao X, Pan Z. Salmonella Enteritidis GalE protein inhibits LPS-induced NLRP3 inflammasome activation. *Microorganisms.* 2022 Apr 26;10(5):911. doi:10.3390/microorganisms10050911.

Hyman P. Phages for phage therapy: isolation, characterization, and host range breadth. *Pharmaceuticals.* 2019;12(1):35. doi:10.3390/ph12010035.

Hyman P, Abedon ST. Bacteriophage host range and bacterial resistance. *Adv Appl Microbiol.* 2010;70:217–248. doi:10.1016/S0065-2164(10)70007-1.

Issenhuth-Jeanjean S, Roggentin P, Mikoleit M, Guibourdenche M, de Pinna E, Nair S, Fields PI, Weill FX. Supplement 2008–2010 (no. 48) to the White-Kauffmann-Le Minor scheme. *Res Microbiol.* 2014;165(7):526–530.

Islam MS, Zhou Y, Liang L, Nime I, Liu K, Yan T, Wang X, Li J. Application of a phage cocktail for control of Salmonella in foods and reducing biofilms. *Viruses.* 2019;11(9):841. doi:10.3390/v11090841.

Jajere SM. A review of Salmonella enterica with particular focus on the pathogenicity and virulence factors, host specificity and antimicrobial resistance including multidrug resistance. *Vet World.* 2019;12(4):504–521. doi:10.14202/vetworld.2019.504-521.

Jończyk E, Kłak M, Międzybrodzki R, Górski A. The influence of external factors on bacteriophages—review. *Folia Microbiol (Praha).* 2011;56(3):191–200. doi:10.1007/s12223-011-0039-8.

Jurczak-Kurek A, Gąsior T, Nejman-Faleńczyk B, Bloch S, Dydecka A, Topka G, Necel A, Jakubowska-Deredas M, Narajczyk M, Richert M, Mieszkowska A, Wróbel B, Węgrzyn G, Węgrzyn A. Biodiversity of bacteriophages: morphological and biological properties of a large group of phages isolated from urban sewage. *Sci Rep.* 2016 Oct 4;6:34338. doi:10.1038/srep34338.

Kamada N, Seo SU, Chen GY, Núñez G. Role of the gut microbiota in immunity and inflammatory disease. *Nat Rev Immunol.* 2013;13(5):321–335. doi:10.1038/nri3430.

Kardong KV. *Vertebrates: comparative anatomy, function, evolution.* 2nd ed. New York: McGraw-Hill; 1998.

Kestra-Gounder AM, Tsolis RM, Bäumlér AJ. Now you see me, now you don't: the interaction of *Salmonella* with innate immune receptors. *Nat Rev Microbiol.* 2015 Apr;13(4):206–216. doi:10.1038/nrmicro3428.

Kutter E, Sulakvelidze A, editors. *Bacteriophages: Biology and Applications.* Boca Raton: CRC Press; 2004.

Lin DM, Koskella B, Lin HC. Phage therapy: an alternative to antibiotics in the age of multi-drug resistance. *World J Gastrointest Pharmacol Ther.* 2017 Aug 6;8(3):162–173. doi:10.4292/wjgpt.v8.i3.162.

Liu R, Han G, Li Z, et al. Bacteriophage therapy in aquaculture: current status and future challenges. *Folia Microbiol.* 2022;67:573–590. doi:10.1007/s12223-022-00965-6.

Ly-Chatain MH. The factors affecting effectiveness of treatment in phage therapy. *Front Microbiol.* 2014;5:51. doi:10.3389/fmicb.2014.00051.

Loc-Carrillo C, Abedon ST. Pros and cons of phage therapy. *Bacteriophage.* 2011 Mar;1(2):111–114. doi:10.4161/bact.1.2.14590.

Mahmoud M, Askora A, Barakat AB, Rabie OEF, Hassan SE. Isolation and characterization of polyvalent bacteriophages infecting multidrug-resistant *Salmonella* serovars isolated from broilers in Egypt. *Int J Food Microbiol.* 2018;266:8–13. doi:10.1016/j.ijfoodmicro.2017.11.009.

Moye ZD, Woolston J, Sulakvelidze A. Bacteriophage applications for food production and processing. *Viruses.* 2018;10(4):205. doi:10.3390/v10040205.

Nováček J, Šiborová M, Benešik M, Pantůček R, Doškař J, Plevka P. Structure and genome release of Twort-like Myoviridae phage with a double-layered baseplate. *Proc Natl Acad Sci U S A.* 2016 Aug 16;113(33):9351–9356. doi:10.1073/pnas.1605883113.

Odey TOJ, Tanimowo WO, Afolabi KO, et al. Antimicrobial use and resistance in food animal production: food safety and associated concerns in Sub-Saharan Africa. *Int Microbiol.* 2024;27:1–23. doi:10.1007/s10123-023-00462-x.

Oechslin F. Resistance development to bacteriophages occurring during bacteriophage therapy. *Viruses.* 2018;10(7):351. doi:10.3390/v10070351.

Organização Mundial da Saúde (OMS). *Salmonella (non-typhoidal): fact sheet.* Geneva: OMS; 2023. Available from: [https://www.who.int/news-room/fact-sheets/detail/salmonella-\(non-typhoidal\)](https://www.who.int/news-room/fact-sheets/detail/salmonella-(non-typhoidal)). Accessed 25 Jan 2026.

Payne RJH, Jansen VAA. Pharmacokinetic principles of bacteriophage therapy. *Clin Pharmacokinet.* 2003;42(4):315–325. doi:10.2165/00003088-200342040-00002.

Pereira C, Moreirinha C, Lewicka M, Almeida P, Clemente C, Cunha Â, Delgadillo I, Romalde JL, Nunes ML, Almeida A. Bacteriophages with potential to inactivate *Salmonella* Typhimurium: use of single phage suspensions and phage cocktails. *Virus Res.* 2016 Jul 15;220:179–192. doi:10.1016/j.virusres.2016.04.020.

Phothaworn P, Supokaivanich R, Lim J, Klumpp J, Imam M, Kutter E, Galyov EE, Dunne M, Korbsrisate S. Development of a broad-spectrum Salmonella phage cocktail containing Viunalike and Jerseylike viruses isolated from Thailand. *Food Microbiol.* 2020 Dec;92:103586. doi:10.1016/j.fm.2020.103586.

Porwollik S, Boyd EF, Choy C, Cheng P, Florea L, Proctor E, McClelland M. Characterization of *Salmonella enterica* subspecies I genovars by use of microarrays. *J Bacteriol.* 2004 Sep;186(17):5883–5898. doi:10.1128/JB.186.17.5883-5898.

Ramsey J, Rasche H, Maughmer C, Criscione A, Mijalis E, Liu M, Hu JC, Young R, Gill JJ. Galaxy and Apollo as a biologist-friendly interface for high-quality cooperative phage genome annotation. *PLoS Comput Biol.* 2020;16(11):e1008214. doi:10.1371/journal.pcbi.1008214.

Rastegar S, Skurnik M, Tadjrobehkar O, Samareh A, Samare-Najaf M, Lotfian Z, Khajedadian M, Hosseini-Nave H, Sabouri S. Synergistic effects of bacteriophage cocktail and antibiotics combinations against extensively drug-resistant *Acinetobacter baumannii*. *BMC Infect Dis.* 2024 Oct 26;24(1):1208. doi:10.1186/s12879-024-10081-0.

Ribas A, Poonlaphdecha S. Wild-caught and farm-reared amphibians are important reservoirs of *Salmonella*: a study in north-east Thailand. *Zoonoses Public Health.* 2017 Mar;64(2):106–110. doi:10.1111/zph.12286.

Richards GP. Bacteriophage remediation of bacterial pathogens in aquaculture: a review of the technology. *Bacteriophage.* 2014;4(4):e975540. doi:10.4161/21597081.2014.975540.

Rodrigues RA. Ocorrência de *Salmonella* spp. em carcaças e vísceras de rãs (*Rana catesbeiana* – rã-touro): avaliação do processo de abate [dissertation]. Botucatu: Universidade Estadual Paulista (UNESP); 2007.

Rodriguez A, Pangloli P, Richards HA, Mount JR, Draughon FA. Prevalence of Salmonella in diverse environmental farm samples. *J Food Prot.* 2006 Nov;69(11):2576–2580. doi:10.4315/0362-028X-69.11.2576.

Sillankorva SM, Oliveira H, Azeredo J. Bacteriophages and their role in food safety. *Int J Microbiol.* 2012;2012:863945. doi:10.1155/2012/863945.

Silva EC, Dias SC, Costa PC, Tiba MR, et al. Profile of Salmonella isolates in bullfrog production: PFGE, MLST and antimicrobial resistance. *J Food Prot.* 2025 Aug;88(8):100550. doi:10.1016/j.jfp.2025.100550.

Sommer F, Bäckhed F. The gut microbiota—masters of host development and physiology. *Nat Rev Microbiol.* 2013;11(4):227–238. doi:10.1038/nrmicro2974.

Sorensen AN, Brondsted L. Renewed insights into Ackermannviridae phage biology and applications. *npj Viruses.* 2024;2:37. doi:10.1038/s44298-024-00046-0.

Spricigo DA, Bardina C, Cortés P, Llagostera M. Use of a bacteriophage cocktail to control Salmonella in food and the food industry. *Int J Food Microbiol.* 2013 Jul 15;165(2):169–174. doi:10.1016/j.ijfoodmicro.2013.05.009.

Srinivasiah S, Bhavsar J, Thapar K, Liles M, Schoenfeld T, Wommack KE. Phages across the biosphere: contrasts of viruses in soil and aquatic environments. *Res Microbiol.* 2008 Jun;159(5):349–357. doi:10.1016/j.resmic.2008.04.010.

Sulakvelidze A, Alavidze Z, Morris JG Jr. Bacteriophage therapy. *Antimicrob Agents Chemother.* 2001 Mar;45(3):649–659. doi:10.1128/AAC.45.3.649-659.2001.

Sulakvelidze A. Using lytic bacteriophages to eliminate or significantly reduce contamination of food by foodborne bacterial pathogens. *J Sci Food Agric.* 2013;93(13):3137–3146. doi:10.1002/jsfa.6222.

Svircev A, Roach D, Castle A. Framing the future with bacteriophages in agriculture. *Viruses*. 2018 Apr 25;10(5):218. doi:10.3390/v10050218.

Switt AI, Sulakvelidze A, Wiedmann M, Kropinski AM, Wishart DS, Poppe C, Liang Y. Salmonella phages and prophages: genomics, taxonomy, and applied aspects. *Methods Mol Biol*. 2015;1225:237–287. doi:10.1007/978-1-4939-1625-2_15.

Unverdi A, Erol HB, Kaskatepe B, Babacan O. Characterization of Salmonella phages isolated from poultry coops and its effect with nisin on food bio-control. *Food Sci Nutr*. 2024 Jan 9;12(4):2760–2771. doi:10.1002/fsn3.3956.

Vieira RHSF, Teixeira AA, Costa RA, Carvalho EMR, Fonteles Filho AA. Microbiological quality of fresh sausage made from frog meat during storage under different packaging conditions. *Food Sci Technol (Campinas)*. 2014;34(1):7–13. doi:10.1590/S0101-20612014005000004.

Weigel C, Seitz H. Bacteriophage replication modules. *FEMS Microbiol Rev*. 2006 May;30(3):321–381. doi:10.1111/j.1574-6976.2006.00015.x.

Wiggins BA, Alexander M. Minimum bacterial density for bacteriophage replication: implications for significance of bacteriophages in natural ecosystems. *Appl Environ Microbiol*. 1985 Jan;49(1):19–23. doi:10.1128/aem.49.1.19-23.1985.

Wittebole X, De Roock S, Opal SM. A historical overview of bacteriophage therapy as an alternative to antibiotics for the treatment of bacterial pathogens. *Virulence*. 2014;5(1):226–235. doi:10.4161/viru.25991.

Woodhams DC, Bletz M, Kueneman J, McKenzie V. Managing amphibian disease with skin microbiota. *Trends Microbiol*. 2016;24(3):161–164. doi:10.1016/j.tim.2015.12.010.

Woo PTK, Bruno DW, editors. Fish diseases and disorders. Volume 3: Viral, bacterial and fungal infections. 2nd ed. Wallingford: CABI; 2011.

Yoo S, Lee KM, Kim N, Vu TN, Abadie R, Yong D. Designing phage cocktails to combat the emergence of bacteriophage-resistant mutants in multidrug-resistant *Klebsiella pneumoniae*. *Microbiol Spectr*. 2024;12(1):e0125823. doi:10.1128/spectrum.01258-23.

Young R. Phage lysis: do we have the hole story yet? *Curr Opin Microbiol*. 2013 Dec;16(6):790–797. doi:10.1016/j.mib.2013.08.008.

Zhang M, Song Q, Liu Z, Clokie MRJ, Sicheritz-Pontén T, Petersen B, Wang X, Zhang Q, Xu X, Luo Y, Lv P, Liu Y, Li L. Design of lytic phage cocktails targeting *Salmonella*: synergistic effects based on *in vitro* lysis, *in vivo* protection, and biofilm intervention. *Viruses*. 2025 Oct 12;17(10):1363. doi:10.3390/v17101363.

Zulk JJ, Clark JR, Ottinger S, Ballard MB, Mejia ME, Mercado-Evans V, Heckmann ER, Sanchez BC, Trautner BW, Maresso AW, Patras KA. Phage resistance accompanies reduced fitness of uropathogenic *Escherichia coli* in the urinary environment. *mSphere*. 2022 Aug 31;7(4):e0034522. doi:10.1128/msphere.00345-22.